Journal Pre-proof

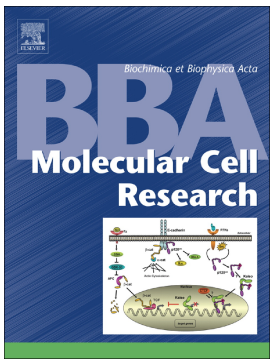

Oxidative stress induces transcription of telomeric repeat-containing RNA (TERRA) by engaging PKA signaling and cytoskeleton dynamics

Natalia M. Galigniana, Nancy L. Charó, Romina Uranga, Ana María Cabanillas, Graciela Piwien-Pilipuk

PII: S0167-4889(20)30001-X

DOI: https://doi.org/10.1016/j.bbamcr.2020.118643

Reference: BBAMCR 118643

To appear in: *BBA - Molecular Cell Research*

Received date: 12 August 2019

Revised date: 27 December 2019

Accepted date: 2 January 2020

Please cite this article as: N.M. Galigniana, N.L. Charó, R. Uranga, et al., Oxidative stress induces transcription of telomeric repeat-containing RNA (TERRA) by engaging PKA signaling and cytoskeleton dynamics, *BBA - Molecular Cell Research*(2020), https://doi.org/10.1016/j.bbamcr.2020.118643

This is a PDF file of an article that has undergone enhancements after acceptance, such as the addition of a cover page and metadata, and formatting for readability, but it is not yet the definitive version of record. This version will undergo additional copyediting, typesetting and review before it is published in its final form, but we are providing this version to give early visibility of the article. Please note that, during the production process, errors may be discovered which could affect the content, and all legal disclaimers that apply to the journal pertain.

© 2020 Published by Elsevier.

Oxidative stress induces transcription of telomeric repeat-containing RNA (TERRA) by engaging PKA signaling and cytoskeleton dynamics

Natalia M. Galigniana[a], Nancy L. Charó[a], Romina Uranga[b], Ana María Cabanillas[c], Graciela Piwien-Pilipuk[a*]

(a) Laboratory of Nuclear Architecture, Instituto de Biología y Medicina Experimental (IByME-CONICET), Ciudad Autónoma de Buenos Aires, Argentina.

(b) Instituto de Investigaciones Bioquímicas de Bahía Blanca (IIBBB-CONICET); Departamento de Biología, Bioquímica y Farmacia, Universidad Nacional del Sur, Bahía Blanca, Argentina.

(c) Centro de Investigaciones en Bioquímica Clínica e Inmunología (CIBICI-CONICET); Departamento de Bioquímica Clínica, Facultad de Ciencias Químicas, Universidad Nacional de Córdoba, Córdoba, Argentina.

Journal Pre-proof

*****Corresponding author:

Graciela Piwien-Pilipuk: Laboratory of Nuclear Architecture, Instituto de Biología y Medicina Experimental (IByME-CONICET), Vuelta de Obligado 2490, C1428ADN, Ciudad Autónoma de Buenos Aires, Argentina. Phone number: +54- 11-4783-2869 Fax: +54-11-4786-2564
E-mail address: gpiwien@conicet.gov.ar

Abstract

Long non-coding RNAs transcribed from telomeres, known as TERRA (telomeric repeat-containing RNA), are associated with telomere and genome stability. TERRA abundance responds to different cell stresses; however, no studies have focused on oxidative stress, condition that damages biomolecules and is involved in aging and disease. Since telomeres are prone to oxidative damage leading to their dysfunction, our objective was to characterize TERRAs and the mechanisms that control their expression. TERRA increased in cells exposed to H_2O_2 and reverted by antioxidant treatment. TERRAs are also induced in brown adipose tissue of mice exposed to cold, which raises mitochondrial ROS. In cells exposed to H_2O_2, ChIP showed that chromatin landscape was modified favoring telomere transcription. TERRAs interacted with HP1α/γ, proteins that were found recruited to subtelomeres. Since HP1γ interacts with the transcriptional machinery, TERRAs may stimulate their own expression by recruiting HP1γ to subtelomeres. TERRA induction reverted within 2h after removal of H_2O_2 from culture medium, suggesting they have protective functions. This was supported by rapid TERRA induction following a second H_2O_2 challenge. PKA inhibitors H89 and PKI blocked TERRA increase by H_2O_2 or IBMX+Forskolin treatment, suggesting PKA signaling regulates TERRA induction. Treatment of cells with drugs that disturb cytoskeleton integrity or growing cells on surfaces of different stiffness known to generate differential cytoskeleton tension also modified TERRA levels and sensitized cells to lower H_2O_2 concentrations. In summary, we show that TERRAs are induced in response to oxidative stress and are regulated by PKA as well as by changes in cytoskeleton dynamics.

Key words: TERRA, oxidative stress, telomere dysfunction, transcriptional memory, PKA, cytoskeleton dynamics.

Abbreviations: ncRNA: non-coding RNA; lncRNA: long non-coding RNA; sncRNA: small non-coding RNA; TERRA: telomeric repeat-containing RNA; ALT: alternative lengthening of telomeres; ROS: reactive oxygen species; NAC: N-acetyl-L-cysteine; UCP-1: uncoupling protein-1; TAF: telomere-associated DNA damage foci; HP1: heterochromatin protein 1; H_2O_2: hydrogen peroxide; $NaAsO_2$: sodium arsenite; TIAR: TIA-1 related protein; WB: Western blot; IP: immunoprecipitation; IIF: indirect

Journal Pre-proof

immunofluorescence; ChIP: chromatin immunoprecipitation; RIP: RNA immunoprecipitation; H3K9me3: trimethylation on Lys9 of histone H3; p-Ser5 RNA pol II: RNA polymerase II phosphorylated at Ser5; H4Ac: acetylated histone H4; Nup62: nucleoporin 62; NPC: nuclear pore complex; P-Thr198 PKA: PKA phosphorylated at Thr198; LINC: linker of nucleoskeleton and cytoskeleton; E: elastic modulus; HS: horse serum; CSD: chromoshadow domain.

Journal Pre-proof

1. INTRODUCTION

Eukaryotic genomes possess intragenic and intergenic sequences that give rise to non-coding RNAs (ncRNAs) that have been linked to cellular processes in physiology and disease [1]. Different criteria have emerged in order to classify the ever-growing list of identified ncRNAs, including length, transcript properties, location with respect to known genomic annotations or regulatory elements, and function [2]. The most basic criterion classifies them according to their length into small (sncRNA) and long ncRNAs (lncRNA). Active transcription of telomeres gives rise to a member of the long class of ncRNAs known as telomeric repeat-containing RNAs (TERRA) [3, 4]. The C-rich strand of telomeres is transcribed by the RNA polymerase II, generating TERRA transcripts composed of subtelomeric sequences and a variable number of the telomeric UUAGGG-repeat, which causes TERRA populations to be heterogeneous in size, ranging from 100bp to 9kb, sustaining several important functions at chromosome ends [3-5]. They have been shown to be novel structural components of telomeres [3, 4], where they participate in heterochromatin formation and favor capping of these structures by the protein complex shelterin. They can also interact with telomerase, possibly favoring its activity *in vivo* by recruiting telomerase at short telomeres [6, 7] and by preventing the accumulation of the telomerase-inhibiting hnRNPA1 at telomeres [6], although there is evidence that TERRA overexpression in human cancer cells does not affect telomerase activity[8]. Other enzymes that localize at telomeres, such as methyltransferase Suv39H1 and the member of the NuA2 histone acetyltransferase complex MORF4L2, have also been identified as TERRA-binding proteins, favoring their recruitment to telomeres [9]. Furthermore, at dysfunctional ultrashort telomeres, TERRAs can base-pair with their template DNA strand to form RNA:DNA hybrid structures known as R-loops that favor homologous recombination of telomeres, thus promoting alternative lengthening of telomeres (ALT) and delaying senescence in telomerase-negative cells [9].

TERRA abundance is modified in response to a variety of conditions, including telomere epigenetic status [4, 10-14], cell cycle phase [15], development [4, 16], nuclear reprogramming [17, 18], as well as in diseases such as cancer [19]. It has also been described that TERRA levels are differentially modulated in response to different cell stresses. TERRA levels decrease in cells exposed to UV-C radiation [20]. In contrast, heat shock increases TERRA expression [4]. However, to our knowledge, it is not known whether TERRAs are modulated in response to oxidative stress. It is important to gain insight in the underlying mechanisms that control TERRA expression in this context, since oxidative stress is relevant in ageing [21] as well as in a plethora of diseases, including

neurodegenerative diseases [22]; cardiovascular disease [23]; obesity, a pathology in which increased production of reactive oxygen species (ROS) in the adipose tissue may underlie occurrence of insulin resistance [24-27]; as well as in cancer [28]. The tumor-associated inflammatory response favors tumor progression by secreting bioactive molecules to the tumor microenvironment, as well as by secreting ROS that activate signaling cascades, like MAPK/AP-1 and NF-κB, and are mutagenic for nearby cells, accelerating their transformation [28, 29].

For a long time, ROS have only been considered harmful, and thus detrimental for the cell. However, ROS have proven to be signaling molecules, and it is well accepted that a lack of necessary ROS can also be harmful. As signaling molecules, ROS participate in the control of diverse essential cellular processes ranging from cell survival, proliferation, migration, up to cell differentiation [30]. For example, activation of brown adipose tissue (BAT) thermogenesis is accompanied by increased levels of mitochondrial ROS. Treatment of mice with the cell permeable antioxidant N-acetyl-L-cysteine (NAC) or with the mitochondria-targeted antioxidant MitoQ caused severe hypothermia when mice were exposed to cold, suggesting that elevated ROS is required for increasing uncoupling protein (UCP)1-dependent respiration for proper thermogenesis [31]. In the presence of elevated ROS, both protein thiols and glutathione pools became substantially oxidized during thermogenic respiration in BAT of mice exposed to cold [31-33]. One key target is the Cys253 of UCP-1, whose oxidation drives increased thermogenic respiration in BAT [31]. Importantly, the redox changes that take place in BAT upon cold exposure are dynamic, reversible and precisely controlled by thiol antioxidant pathways [34] since uncontrolled ROS can be detrimental to the cell. Therefore, when a redox imbalance results in an excess of ROS, the cell faces oxidative stress that leads to a disruption of redox signaling and/or molecular damage that triggers diverse mechanisms that lead to survival (if the stress situation is overcome) or to cell death [30, 35, 36].

ROS are reactive towards lipids, proteins and nucleic acids, and their excess results in damage to cell structure and functions. In particular, it has been shown that telomeres are more susceptible to suffer DNA damage by ROS than other regions of the genome. Indeed, the triplet guanines in the telomeric TTAGGG-repeats confer high oxidative reactivity and the resulting oxidative guanine lesions result in telomere configurations that decrease DNA repair efficiency [37]. Interestingly, it has been shown that telomeres form atypical aggregates of varied size and number in tumor cell nuclei and in cells conditionally overexpressing c-Myc [38]. These changes could be attributed, at least in part, to the fact that c-Myc overexpression alters the nuclear matrix [39, 40] which would facilitate recombination and/or fusion events, as well as the formation of telomeric

aggregates [38]. Furthermore, c-Myc activation induces DNA damage mediated by increased ROS production, where antioxidant treatment lowers ROS levels and prevents DNA damage [41]. It was also shown that chronic inflammation in mice induces telomere dysfunction due to ROS overproduction *via* COX-2, which is blocked by anti-inflammatory or antioxidant treatment [42]. Therefore, since an oxidative context leaves telomeres prone to damage and abnormal aggregation, we hypothesize that the expression of TERRA transcripts will increase possibly for telomere protection. In the present study, our results show that oxidative stress, generated by exposing cells to H_2O_2 or $NaAsO_2$, induces TERRA expression, which is blocked by the antioxidant NAC. Importantly, TERRAs are induced *in vivo* in BAT, tissue in which ROS increase when mice are exposed to cold. TERRA induction is reversible, suggesting they play a protective role at telomeres. In fact, epigenetic changes at subtelomeric chromatin that favors TERRA transcription after an initial exposure to H_2O_2 persists in cells, leading to faster TERRA induction in a subsequent oxidative challenge. We found TERRAs could participate in these chromatin state changes by interacting with the heterochromatin protein 1 (HP1) family proteins HP1α and HP1γ, the latter being a novel TERRA-binding isoform. Finally, we identified PKA signaling and cytoskeleton integrity to be relevant mechanisms involved in the regulation of TERRA induction.

Journal Pre-proof

2. MATERIALS AND METHODS

2.1 Antibodies. Mouse monoclonal IgG against HP1γ (clone 42s2), mouse monoclonal IgG against HP1α (clone 15.19s2), and anti-acetylated histone H4 were from EMD Millipore. Anti-α-tubulin, anti-TRF1 and ChIP-grade antibodies against HP1γ (rabbit polyclonal IgG), histone H3K9me3 and actin were from Abcam (Cambridge, UK). Nups mouse monoclonal IgG and P-Ser5 RNA pol II mouse monoclonal IgM (clone H14) antibodies were from Covance (New Jersey, USA), while IgG anti-IgM antibody was from Upstate-Millipore (Billerica, MA, USA). Mouse monoclonal IgG anti-TIAR was from BD Transduction Laboratories, rabbit monoclonal IgG against pan-actin was from Epitomics and P-Thr198 PKA catalytic subunits α/β/γ was from Santa Cruz Biotechnology. Lamin A/C, PKA catalytic subunit α and P-Ser139 γH2AX were from Cell Signaling. HRP-conjugated goat anti-rabbit, phalloidin-FITC, and mouse IgG anti-Flag M2 (non-immune serum) were from Sigma-Aldrich. HRP-conjugated goat anti-mouse was from Amersham Biosciences (Little Chalfont, UK). Rabbit IgG anti-GST epitope tag (non-immune serum) was purchased from Affinity BioReagents (Golden, CO). Secondary antibodies labeled with Alexa-Fluor 488 dyes were purchased from Molecular Probes (Eugene, OR, USA). Rhodamine-labeled goat anti-rabbit IgG and HRP-conjugated goat anti-mouse IgM were purchased from Jackson ImmunoResearch (West Grove, PA, USA). HRP-conjugated protein A was purchased from Calbiochem.

2.2 Cell culture and reagents. Dulbecco's modified Eagle's medium (DMEM), trypsin-EDTA, fetal bovine serum (FBS) and calf serum (CS) were purchased from Gibco Life Technologies – Invitrogen, (Carlsbad, CA, USA). Human embryonic kidney HEK-293T cells and C2C12 mouse myoblasts were obtained from the American Type Culture Collection (ATCC). HEK-293T cells were grown in DMEM 4.5 g/liter glucose and supplemented with 10% v/v CS and C2C12 cells were grown in DMEM 4.5 g/liter glucose and supplemented with 10% v/v FBS in a humidified 5% CO_2 atmosphere at 37°C. C2C12 cells were grown until confluence in DMEM 10% FBS, and then changed to DMEM 2% horse serum (HS) during 4 days for induction of differentiation, as previously described [43]. For exposure to oxidative agents, we used hydrogen peroxide (H_2O_2) solution 30% (w/w) in water from Sigma-Aldrich (St. Louis, MO, USA)., while buthionine sulfoximine (Sigma-Aldrich) and sodium arsenite (Mallinckrodt) were prepared in distilled water, and the final working concentrations are indicated in each experiment. N-acetyl-L-cysteine (NAC) was purchased from Sigma-Aldrich, stock solutions were prepared in distilled water and used at a 5mM final concentration. Cells were pre-incubated 30 min with 5 mM NAC before adding an oxidative agent. For cytoskeleton integrity experiments, colcemid

(Sigma-Aldrich) and paclitaxel (LC Laboratories) stock solutions were prepared in DMSO and used at final concentrations of 0.6µg/ml and 1µM, respectively. For PKA signaling evaluation, 3-isobutyl-1-methylxanthine (IBMX), forskolin and PKI were purchased from Sigma-Aldrich, and H89 dihydrochloride salt was from LC Laboratories. IMBX stock solution was dissolved in distilled water and used at a final concentration of 52µM in combination with forskolin 30µM. The PKA inhibitor H89 dihydrochloride salt was resuspended in DMSO and used at a 20µM final concentration, and PKI was resuspended in distilled water and used at a 0.5µM final concentration. For trypan blue staining, cells were trypsinized, spun down, resuspended in culture medium and incubated at room temperature with trypan blue solution at a final concentration of 0.2% (w/v). The proportion of viable cells (non-stained) was determined in a Neubauer chamber.

2.3 Cell fractionation and Western blot (WB) analysis. Cell fractionation was performed as previously described [43]. Briefly, cells were either left untreated or treated 4h with 500 µM H_2O_2. Cells were then washed twice with PBS and once with ice-cold hypotonic buffer (20 mM HEPES, 1 mM EDTA y 1 mM EGTA). Cells were harvested in hypotonic buffer containing 0.2% NP40 plus protease inhibitors, dounced 50 times with a loose pestle on ice and centrifuged 30 s at 13500 rpm. The supernatant (cytosol) was separated and stored at -80°C, while the nuclear pellets were lysed in lysis buffer (50 mM Tris/HCl pH 7,5, 120 mM NaCl, 1 mM EDTA, 6 mM EGTA, 0,1% NP40) plus protease inhibitors for IP experiments, or in TRIzol reagent for TERRA assessment. Total, cytosolic and nuclear fractions were resolved by SDS-PAGE and analyzed by immunoblotting, as previously described [43-45].

2.4 Immunoprecipitation (IP) assays. IPs were performed as we previously described [43, 44]. HRP-conjugated protein A was used for immunoblotting.

2.5 Indirect immunofluorescence (IIF) assays. IIF was performed as previously described [43-45]. Briefly, cells were grown on coverslips, incubated in the absence or the presence of 500µM H_2O_2 for 4h or treated as indicated in figure legends, and then fixed 10 min in 2% PFA+2% sucrose in PBS, followed by 10 min in 4% PFA+4% sucrose in PBS at room temperature. Quenching of cellular autofluorescence was performed by incubating 10 min in a 10 mM NH_4Cl solution in PBS. Cells were permeated by incubating 10 min in 0.1% Triton X-100 in PBS. Coverslips were washed three times with PBS, blocked 1h with blocking buffer (1% bovine serum albumin in PBS), and incubated O.N. with the primary antibodies indicated in figure legends. After 1h incubation with the secondary antibodies labeled with Alexa-488 or rhodamine, nuclei were stained with DAPI and coverslips were

mounted in Vectashield mounting medium. All IIF conditions were tested to avoid non-specific reactions using only the secondary antibodies. Laser-scanning confocal microscopy was performed with the Olympus Fluoview FV10i.

2.6 Image analysis. *Software Fiji-Image J program* (v. 1.45s) from the NIH was utilized for all image analyses. To quantify co-localization events, the *Colocalization* plug-in was used. To measure fluorescence intensity of DNA damage foci, the *Integrated Intensity* was included as a measurement in the ROI Manager. In both cases, at least 30 nuclei were analyzed. Profiles of band intensities of agarose gels were obtained using the *Plot profile* plug-in.

2.7 RNA extraction and PCR analysis. RNA was isolated with TRIzol reagent (TRI Reagent, Sigma-Aldrich) following the manufacturer's instructions. DNAse I treatment was performed using the RQ1 RNase-Free DNase kit from Promega. For cDNA synthesis, M-MLV Reverse Transcriptase from Promega was used. End-point PCR was performed using TERRA primers previously reported by Azzalin *et al*. [3]: initial denaturation 4 min 94°C; 35 cycles of 30 s 94°C, 30 s 57°C and 30 s 72°C; final elongation 10 min 72°C. qPCR was performed using human and mouse TERRA primers previously reported by Deng *et al.* [19, 46]: activation of FastStart Taq DNA Polymerase 10 min 95°C, 40 cycles of 15 s 95°C and 1 min 60°C; dissociation curve.

2.8 Chromatin immunoprecipitation (ChIP) and re-ChIP assays. ChIP was performed as previously described [43, 45]. The primers for the 17p subtelomeric region used for PCR amplification were the same as those previously reported [3]. Re-ChIP assays were performed as described [43] using 5µg of anti-HP1γ for the first IP and 5µg of either anti-Nups or anti-actin for each of the second IPs.

2.9 RNA Immunoprecipitation assay (RIP). To study TERRA interaction with HP1 proteins, we followed a protocol adapted from Selth *et al*. [47]. Briefly, cells were crosslinked as in ChIP assays, washed in PBS, scraped with PBS plus protease inhibitors and nuclei were isolated in hypotonic buffer (20mM HEPES, 1mM EDTA y 1 mM EGTA, 0.2% NP40) plus 40 U/ml RNAse OUT (Invitrogen-Thermo Fisher Scientific) and protease inhibitors, douncing 50 times with a loose pestle. Pelleted nuclei were resuspended in RIP buffer (150mM KCl, 25mM Tris–HCl pH 7.4, 5mM EDTA, 0.5mM DTT, 0.5% NP40) plus 40 U/ml RNAse OUT and protease inhibitors, and dounced 50 times with a tight pestle. Samples were centrifuged, and supernatants containing proteins, RNA and genomic DNA were sonicated in a Biodisruptor from Diagenode. RNA was quantified in a Nanodrop2000 and 6mg of RNA was used for each IP using 5µg of either immune or non-immune antibody, incubated O.N. at

4°C with rotation. IP samples were incubated with protein A/G agarose (Sigma-Aldrich), eluted for 10 min at 37°C in elution buffer (10 mM EDTA, 100mM Tris–HCl pH 8.0, 1% SDS) plus 40 U/ml RNAse OUT and the resulting supernatants were treated 1h at 42°C with proteinase K and decrosslinked 1h at 65°C, including input RNA. TRIzol was added to isolate RNA following the manufacturer's instructions.

2.10 Polyacrylamide hydrogels. Polyacrylamide solutions corresponding to Young's modulus (E) 60 kPa or 1.05 kPa were prepared by mixing 40% acrylamide, 2% bis-acrylamide, water, and 10% APS solution according to the volumes previously reported [48]. We then followed the protocol described by Worthen *et al.* [49].

2.11 Cold exposure of male C57BL/6J mice. Mice were left at room temperature or placed in cages at 4°C during 4h before euthanasia by cervical dislocation. Interscapular, epididymal and inguinal fat depots were surgically removed as described [31]. Animal experiments were performed according to procedures approved by CICUAL – IBYME.

2.12 Statistical Analysis. Single comparisons were performed using two-tailed Student's t-test and multiple comparisons by one-way ANOVA followed by *post hoc* Tukey's test using GraphPad Prism 6.

Journal Pre-proof

3. RESULTS

3.1 *Oxidative stress induces TERRA expression.*

TERRAs are known to participate in telomere protection. In order to test whether oxidative stress induces DNA damage at telomeres, we evaluated the effects of H_2O_2 exposure on telomere distribution and whether persistent telomere-associated DNA damage foci (TAF) formed in HEK-293T cells. Telomeres were studied by IIF labeling TRF1, and a punctate staining pattern was observed (**Figure 1A**, panel a), as previously described [50]. When cells were exposed to H_2O_2, the TRF1 signal coalesced (**Figure 1A**, panel e), possibly corresponding to the formation of atypical telomeric aggregates of varied size and number, as previously shown in cells that experience increased ROS levels due to c-Myc overexpression [38, 41]. DNA damage foci were studied by IIF labeling γH2AX, the histone variant H2AX phosphorylated on Ser139 that is found at sites of DNA double strand breaks [51]. The number of γH2AX foci per nucleus increased when HEK-293T cells were exposed to H_2O_2 (**Figure 1A**, panel f vs. b), as expected. We measured both the average number and fluorescence intensity of foci labeled by γH2AX, and we found a significant increase in both parameters (**Figure 1B**). γH2AX co-localization with TRF1 was quantified in order to assess TAF formation, as previously reported [51]. In basal conditions, HEK-293T cells presented a low percentage of TAFs (**Figure 1C** and **Figure 1A** panel c with inset panels 1-2). In contrast, TAF frequencies increased upon H_2O_2 exposure (**Figure 1C** and **Figure 1A**, panel g vs. c, inset panels 1-2). Since TAFs are markers of telomere dysfunction, these results suggest that telomeric DNA undergoes oxidative damage leading to dysfunctional telomeres. Taking in consideration that TERRAs have been shown to protect telomeres, we evaluated their level of expression in HEK-293T cells incubated in the presence of increasing concentrations of H_2O_2. We found that TERRA levels significantly increased upon incubation of cells with 500μM H_2O_2 (**Figure 1D**). Next, TERRA expression was analyzed at different time points of 500μM H_2O_2 treatment. Agarose gels of end-point PCRs, as well as qPCR, show that H_2O_2 induced TERRA expression from chromosomes 17p, 2p, 11q (**Figure 1E**) and chromosomes 2q, 13q, and 17q (**Figure1H**) within 4h of treatment, respectively. In addition, sodium arsenite ($NaAsO_2$), another agent that generates oxidative stress, also increased TERRA levels, as shown for chromosomes 17p, 2p and 11q (**Supplementary Figure S1A**). In order to control that under these conditions cells were in fact exposed to oxidative stress, we evaluated stress granule formation by staining TIA-1 related protein (TIAR) [52]. Stress granules are cytoplasmic complexes of targeted mRNAs and associated proteins that form to stall translation when eukaryotic cells are exposed to stress conditions [53]. As shown in **Figure 1F - panel II**, when cells

were incubated 4h in the presence of 500µM H_2O_2, many TIAR foci were detected by IIF and confocal microscopy. As expected, co-incubation of cells with H_2O_2 and the antioxidant N-acetyl-L-cysteine (NAC) prevented stress granule formation (**Figure 1F**, panel IV vs. II). When TERRA expression was analyzed, we found that the antioxidant NAC blocked the induction of TERRA by H_2O_2, evaluated by both end-point PCR (**Figure 1G**) and qPCR (**Figure 1H**). Furthermore, NAC blocked the induction of TERRA by $NaAsO_2$ treatment (**Supplementary Figure S1B**). Taken together, these results show for the first time that TERRA expression is induced in response to oxidative stress, possibly to protect telomeres from oxidative damage.

It has been recently reported that in BAT, acutely activated thermogenesis increases mitochondrial ROS, whereas it does not occur in white adipose tissue (WAT) [31]. This led us to investigate *in vivo* whether TERRAs transcribed from different chromosomes were induced in BAT, visceral or subcutaneous WAT of C57BL/6J mice exposed 4h to cold (4°C). qPCR analysis of BAT RNA samples showed that cold exposure increased TERRAs expressed from subtelomeres 2q, 5q, 11q and TeloCen between ~4 and almost 7-fold (**Figure 1I**). In contrast, TERRAs were not induced in visceral WAT (**Figure 1I, Epididymal**). Interestingly, subcutaneous WAT, which can undergo a browning process to acquire BAT characteristics upon exposure of mice to cold also have increased mitochondrial ROS, showed a moderate (~1.6-fold) but significant induction of TERRAs (**Figure 1I, Inguinal**). Taken together, these findings show for the first time that TERRA levels increase *in vivo* in response to physiological changes in ROS levels.

3.2 *Oxidative stress induces changes in chromatin landscape at the subtelomeric region*.

Telomeric and subtelomeric regions are enriched in H3K9me3 and H4K20me3, epigenetic marks that are characteristic of heterochromatin, accompanied by underacetylation of histones H3 and H4 [54, 55]. Since telomeres and subtelomeres are endowed with transcriptionally silent marks, we asked whether H_2O_2 exposure of cells modified the chromatin landscape in order to favor TERRA transcription. Thus, we performed chromatin immunoprecipitation (ChIP) assays to analyze methylation of histone H3 and acetylation of histone H4 at the subtelomeric region of chromosome 17p in HEK-293T cells that were incubated 4h in the absence or the presence of H_2O_2. **Figure 2A** shows that H_2O_2 treatment caused an increase in both H3K9me3 (lane 3 vs. 2) and acetylation of histone H4 (lane 11 vs. 10). It is well established that H3K9me3 provides a binding site for the different isoforms of HP1 [56-58]. We found that increased trimethylation of H3K9 was accompanied

by increased recruitment of HP1α (**Figure 2A,** lane 6 vs. 5) at the 17p subtelomeric region, suggesting that chromatin compaction is maintained at subtelomeres when cells are exposed to oxidative stress. However, H3K9me3 has also been shown to be enriched in transcribed regions of active genes in mammalian cells [59], and accordingly we also found increased recruitment of HP1γ (**Figure 2A,** lane 9 vs. 8) to the subtelomeric region. HP1γ interacts with and recruits RNA polymerase II to transcriptionally active sites [43, 59, 60]. We evidenced increased recruitment of RNA polymerase II phosphorylated at Ser5 (p-Ser5 RNA pol II) (**Figure 2A,** lane 14 vs. 13) to the subtelomeric region of chromosome 17p upon H_2O_2 exposure.

It has been recently described that Nups can be targeted to active genes [61, 62]. By performing ChIPs using the monoclonal antibody mAb 414 that recognizes Nups [63, 64], we found they were bound to the 17p subtelomeric region (**Figure 2A**, lane 16), with a low increase caused by treatment of cells with H_2O_2 (**Figure 2A**, lane 17). HP1s are responsible for the recruitment of many chromatin remodelers such as SUVH3 [56-58] and proteins responsible for gene transcription, like the RNA pol II [59], the transcription factor C/EBPβ [45] and nuclear actin [43], among many others [65]. Nups do not have the ability to bind directly to chromatin, thus we analyzed whether HP1s may interact with Nups to possibly facilitate their recruitment to subtelomeres. HP1α and HP1γ were immunoprecipitated from nuclear extracts of HEK-293T cells and complexes were solved by WB. We show for the first time that Nup62 co-immunoprecipitated with HP1γ (**Figure 2B**, lane 2) but not with HP1α (lane 5). The co-immunoprecipitation of Nup62 was specific, since no band was detected when a non-immune serum was used (**Figure 2B**, lanes 1 and 4). P-Ser5 RNA pol II and actin also co-immunoprecipitated with HP1γ (**Figure 2 B**, lane 2) but not with HP1α (lane 5), as previously reported [43, 59]. Importantly, Nup62, as well as actin, co-immunoprecipitated with HP1γ in HEK-293T cells incubated 4h with 500μM H_2O_2 (**Figure 2C**). To obtain evidence that HP1γ and Nups were present in complex associated to the 17p subtelomeric region, re-ChIP assays were performed. Chromatin fragments from HEK-293T cells were immunoprecipitated first with anti-HP1γ, and eluted samples were subjected to a second immunoprecipitation with the antibody mAb 114 that recognizes Nups, followed by purification of these chromatin fragments prior to PCR analysis. We found enrichment of chromatin associated with both proteins at the subtelomeric region of chromosome 17p compared to control non-immune IgG (**Figure 2D,** lane 2 vs. 1), suggesting that complexes containing HP1γ and Nup62 are present in this region. In addition, re-ChIP assays also showed that actin was present in complex with HP1γ (**Figure 2D**, lane 3), as previously shown by others and us for transcribed genes [43, 59]. In summary, when cells were exposed to H_2O_2, both acetylation of histone H4 and H3K9me3

increased, along with binding of HP1α and HP1γ, the latter favoring the recruitment of P-Ser5 RNA pol II, Nup62 and possibly actin, in order to facilitate transcription at subtelomeres when cells are exposed to oxidative stress.

3.3 *TERRA induction by oxidative stress is dynamic.*

To gain insight into the functional role of TERRAs in oxidative stress, we evaluated the subcellular distribution of TERRAs by cell fractionation of cells exposed or not to H_2O_2. We found that the increase in TERRA levels by H_2O_2 was restricted to the nuclear fraction (**Figure 2E**). Since it was previously reported that TERRAs interact with HP1α [66], we investigated whether this nuclear pool of TERRAs could also have the capacity to interact with HP1γ by performing RNA immunoprecipitation (RIP) assays. As shown in **Figure 2F**, TERRA transcribed from the subtelomeric region of chromosome 17p had the ability to interact with HP1γ under basal conditions. A similar result was obtained with HP1α (**Figure 2F**), as previously reported [66]. Interestingly, H_2O_2 treatment of cells increased the interaction of TERRAs with HP1γ in the cell nucleus. To our knowledge, this is the first report showing that TERRAs interact with HP1γ, and it is tempting to speculate that this interaction with HP1s could play a role in controlling TERRA induction when cells have to respond to an oxidative challenge.

In order to further characterize TERRA modulation in response to oxidative stress, we evaluated whether TERRA induction was a dynamic event. To address this question, we treated HEK-293T cells with H_2O_2 during 4h, eliminated the residual H_2O_2, added fresh medium and harvested cells after 15min, 1h, 2h, 4h and 24h had elapsed. The increased levels of TERRA promoted by H_2O_2 treatment began to decrease within 2h of recovery from H_2O_2 exposure (**Figure 3A**, lane 6 vs. 2), reflected in the densitometric analysis of the agarose gel bands of TERRAs from subtelomeres 17p and 2p (**Figure 3B**). After 24h of recovery, TERRA levels appear to be even lower than in control cells (**Figure 3A**, lane 8 vs. 1; **Figure 3B**). To test whether the decrease in TERRA levels was not due to a lower number of viable cells, cell viability was controlled using trypan blue. No changes in cell viability were observed after 24h of recovery following the initial H_2O_2 exposure (**Supplementary Fig. S2**) These results suggest that TERRA expression is dynamic and their induction reverts shortly after the stressor is removed.

It is well known that cells exposed to a stress respond differently when they have to face a second stress [67, 68], however little is known of the mechanism that underlies such differential

responses. To investigate how cells respond to a second oxidative aggression, HEK-293T cells incubated 4h in the presence of H_2O_2 were allowed to recover 24h in fresh culture medium, allowing TERRAs to return to basal levels, and cells were then subjected to a second exposure to H_2O_2 (**Figure 3C**, schematic representation). We found that TERRAs were rapidly induced within 5min, and this induction was sustained up to 1h of the second H_2O_2 treatment (**Figure 3C**, lanes 4-7, and densitometric analysis of TERRA band intensities in **Figure 3D**). This rapid and sustained induction in TERRA levels contrasts with the induction pattern obtained during the first exposure of cells to H_2O_2 (**Figure 1D**). These results prompted us to study whether epigenetic changes and/or modifications in the recruitment of proteins that control transcription at subtelomeres may facilitate the rapid response to the second oxidative insult. Hence, we performed ChIP assays and compared chromatin status in cells exposed 4h to H_2O_2, with cells allowed to recover 24h after an initial exposure to H_2O_2, as well as those that underwent a second 15min treatment with H_2O_2. Interestingly, the enrichment of H3K9me3 and acetylation of histone H4, as well as the binding of HP1α, HP1γ and P-Ser5 RNA pol II observed after 4h H_2O_2 exposure persisted at the subtelomeric region of chromosome 17p through the 24h recovery (**Figure 3E,** lane 4 vs. 3) and was not modified during the second 15min exposure to H_2O_2 (**Figure 3E,** lane 5). Taken together, these results suggest that after the first H_2O_2 exposure, changes in methylation of H3K9, acetylation of H4 and increased binding of HP1α, HP1γ and transcriptionally active RNA pol II are maintained, in order to favor faster TERRA induction when cells are exposed to a second oxidative insult.

3.4 *PKA signaling regulates induction of TERRAs upon oxidative stress*

It has been reported that ROS can activate PKA signaling by a mechanism that does not require an increase in cAMP [69], since increased ROS causes inhibition of adenylate cyclase [70, 71]. Thus, to elucidate the mechanisms underlying TERRA induction in response to oxidative stress, we evaluated whether PKA activation is required for their induction. We found that within 4h of H_2O_2 treatment, PKA activation was evidenced by increased phosphorylation of the catalytic subunit α of PKA on Thr198 (P-Thr198 PKA) (**Figure 4A**) and phosphorylation of HP1γ on Ser 83 (data not shown), a well-known substrate of this kinase [60]. Similar results were obtained when cells were incubated in the presence of IBMX+Forskolin, which increase cAMP by inhibiting phosphodiesterases and by activating adenylate cyclase, respectively (**Figure 4B**). Both phosphorylation of PKA (**Figure 4A, B**) and HP1γ (not shown) induced by H_2O_2 or by IBMX+Forskolin treatment, were blocked by H89, a widely used PKA inhibitor. Next, to determine the importance of PKA signaling in the induction

of TERRA expression, we treated HEK-293T cells with IBMX+Forskolin or H_2O_2 in the absence or presence of H89, and evaluated TERRA levels by qPCR. We found that TERRAs from subtelomeres 2q, 13q and 17q were significantly induced by IBMX+Forskolin treatment (**Figure 4C**), suggesting that activation of the PKA signaling pathway triggers TERRA transcription. Importantly, H89 abrogated the increase in TERRA levels caused by IBMX+Forskolin or H_2O_2 treatment of cells (**Figure 4C**). TERRA induction by H_2O_2 was likewise blocked when PKA inhibition was performed with the cell-permeable PKI (**Figure 4D**). Taken together these results show for the first time that activation of PKA by H_2O_2 is required for the induction of TERRA expression.

3.5 *Cytoskeleton integrity is important for TERRA transcriptional regulation*

Tensional forces sensed by cell-to-cell adhesions and by focal adhesions to the extracellular matrix can be transduced directly into the nucleus along the cytoskeleton, which is connected to the nuclear lamina by the linker of nucleoskeleton and cytoskeleton (LINC) complex. These tensional forces lead to changes in gene expression and cellular functions [72, 73]. It has been reported that ROS affect actin stress fiber formation [74], thus we predicted that changes in the cytoskeleton may be transduced into changes in TERRA transcription. When we stained microtubules in cells exposed to H_2O_2, we evidenced by confocal microscopy that H_2O_2 caused loss of microtubule integrity, which was accompanied by the formation of cytoplasmic α-tubulin aggregates (**Figure 5A**, panel b vs. a), in a similar fashion as cells incubated in the presence of colcemid (panel c), as previously reported [75]. Stress granules stained with anti-TIAR were observed in cells incubated in the presence of H_2O_2 (**Figure 5B**, panel e vs. d) but not when microtubules were disrupted with colcemid (**Figure 5B,** panel f vs. e), supporting the fact that microtubules were disassembled by the action of a different kind of microtubule disrupting agent. As predicted, colcemid treatment also triggered an increase in TERRA levels from chromosomes 17p and 2p assessed by end-point PCR (**Figure 5C**), as we had observed upon H_2O_2 treatment (**Figure 1D**), suggesting that changes in the dynamic organization of microtubules may regulate TERRA transcription. On the other hand, paclitaxel is known to stabilize microtubules in a wide variety of cells by interfering with its dynamic organization [76] and prevents colcemid-induced stress fiber and focal adhesion formation [75]. As such, we decided to explore the possibility that paclitaxel could prevent the effects of H_2O_2 on microtubule integrity, and consequently, block the induction of TERRA expression. However, paclitaxel was not only unable to prevent TERRA induction caused by H_2O_2 treatment of cells (**Figure 5D**, lane 4 vs. 2), but also paclitaxel itself induced TERRA expression from subtelomeres 17p, 2p and 11q (**Figure 5C,** lane 3 vs. 1). Taken

together, these results suggest that changes in the cytoskeleton, either by disassembling or increasing microtubule stability, are possibly sensed by the integrated cytosketelon-nucleoskeleton network, causing an increase in TERRA expression levels.

To further test this possibility, we evaluated TERRA expression in HEK-293Tcells grown on hydrogels of varied stiffness. Altering the properties of the surface to which cells adhere causes significant changes to cell morphology due to cytoskeleton reorganization [48, 77]. The surface stiffness of the polyacrylamide hydrogel is defined by its elastic modulus (E) that has been standardized according to the relative concentrations of acrylamide and bisacrylamide used [48], constituting an ideal tool for studying how changes in cytoskeleton affect TERRA expression. Softer hydrogels confer low resistance to deformation by cells grown on them, leading to rounded cells. On the other hand, stiffer hydrogels are resistant to deformation by cells, resulting in stretched cells. Phase contrast microscopy images show that HEK-293T cells grown on soft hydrogels appear rounded (**Figure 5E,** E=1.05kPa), whereas they are more spread out on stiffer hydrogels (**Figure 5E**, E=60kPa), more similar to cells grown directly on the plastic surface of culture dishes (**Figure 5E**, No gel). qPCR analysis shows that basal TERRA levels decrease as surface stiffness decreases (**Figure 5F**). Importantly, when cells were grown on hydrogels rather than on the plastic surface of the culture dish, TERRA induction took place at a H_2O_2 concentration that was 5 times lower (**Figure 5G**). Taken together, these results provide more evidence that conditions that affect the cytoskeleton can modulate TERRA levels, possibly by means of the integrated cytosketelon-nucleoskeleton network.

In order to further evaluate the possibility that changes in cytoskeleton integrity may play a role in the control of TERRA expression, we analyzed the profile of TERRA expression during the differentiation of C2C12 myoblasts. These cells differentiate into myotubes after 4 days of incubation in DMEM supplemented with 2% horse serum (HS). In this differentiation process, the cytoskeleton undergoes a profound reorganization (**Figure 5H**). In particular, actin is organized into longitudinal continuous filaments in myotubes (**Figure 5H**, panel d vs. c), as has been reported at early stages of sarcomere formation (1-4 days post induction of myoblast differentiation) [43, 78-80]. Furthermore, we measured TERRA levels by qPCR in myoblasts and myotubes and found that TERRAs decreased dramatically when C2C12 myoblasts were induced to differentiate (**Figure 5I**). Hence, C2C12 myoblast differentiation into myotubes, a process in which cytoskeleton reorganization takes place, is accompanied by downregulation of TERRA expression. These results are in line with several recent reports that show there are lower TERRA levels in more differentiated, less proliferative phenotypes

[17-19, 81]. Taken together, our results suggest that a delicate mechanotransduction mechanism may influence TERRA expression, in which deviation from the basal cytoskeleton organization, either due to disruption of microtubules (H_2O_2, colcemid), increased stability of microtubule fibers (paclitaxel) or a generalized reorganization of the cells' cytoarquitecture (hydrogel cultures, C2C12 myoblast differentiation), results in differential TERRA expression.

Journal Pre-proof

DISCUSSION

In the present study, we show for the first time that TERRAs are induced in response to oxidative stress, condition in which we evidenced an increase in TAF frequencies that reflects accumulation of dysfunctional telomeres. Importantly, we observed *in vivo* increase of TERRAs in BAT in response to a physiological increase in mitochondrial ROS that has been proven key for BAT thermogenesis [31, 34]. It is well documented that TERRA abundance is modified during cell cycle phase [15], development [4, 16], nuclear reprogramming [17, 18], as well as in diseases such as cancer [19]. Oxidative stress influences the onset and progression of a plethora of diseases including cancer. Moderate amounts of ROS are useful to cancer since they stimulate stress signaling and add to the mutation burden, thus favoring cancer progression [82]. TERRAs are increased in cancerous tissues [19], and it is possible that augmented ROS may trigger TERRA transcription in these cells. As we mentioned in the introduction, TERRA levels decrease in response to UV-C radiation [20], while TERRA levels are increased in response to heat shock [4]. During the heat shock response, a condition caused by increased protein misfolding and aggregation, ROS are elevated [83]. Thus, it is possible that ROS increased during heat shock may also be responsible for induction of TERRA transcription. Reports also indicate there is an increase of ROS in cells exposed to UV-C radiation, however TERRAs are found downregulated. Thus, despite the fact that different cell stresses may take place with concurrent excess ROS, it is likely that other molecular events participate in the control of TERRA**.** Redox balance is key for cellular homeostasis, since not only oxidative stress but also reductive stress results deleterious [84]. Excess reducing equivalents can lead to a shortage of oxidants that may be necessary to suppress responses that involve protein thiol modification. Reductive stress itself can favor ROS generation by driving mitochondria or other oxidant generators to utilize the abundance of reducing equivalents, and/or by affecting protein folding and endoplasmic reticulum function, processes that also produce ROS, reviewed in [84]. Antioxidant NAC treatment paradoxically promotes an oxidative shift in the cellular redox state. It has been shown that NAC treatment caused reductive stress that lead to impaired mitochondrial function and increased mitochondrial leak of ROS, mainly in the H_2O_2 form [85]. We observed a slight increase in TERRA levels when cells were incubated in the presence of NAC. Thus, it can be speculated that any condition that alters cellular redox homeostasis may trigger TERRA expression in order to protect telomeres.

But why is it relevant to understand the mechanisms that control TERRA transcription in the context of increasing ROS? Telomeric TTAGGG repeats are more prone to oxidative base damage

and repaired less efficiently than non-telomeric TG repeats [37]. Consequently, telomeres require mechanisms for their protection from erosion and loss of telomeric DNA caused by elevated ROS [86-89]. TERRA interact with telomere-associated proteins, including TRF2 and the origin recognition complex (ORC), stabilizing the complex and promoting telomeric heterochromatin, which provides telomere stability [66]. siRNA depletion of TERRAs has been shown to result in dysfunctional telomeres that exhibit loss of H3K9me3 and ORC [66]. In addition, highly transcribed telomeres exhibit high mobility in the interphase nucleus, which could favor the onset of a DNA damage response at dysfunctional telomeres [90]. In fact, we found TERRA levels are markedly increased in cells exposed to H_2O_2 with increased TAFs, but once the aggression disappears, TERRAs are rapidly downregulated. In this scenario, it is tempting to speculate that the dynamic control of TERRAs possibly relies on their protective role facilitating telomeric movement for access to the DNA damage machinery, and/or the maintenance of the heterochromatic structure of telomeres through their interaction with telomere-associated proteins, including HP1α and -γ for maintenance, and even increase of H3K9me3, as shown in this study.

As we already mentioned, elevated ROS that damage DNA, proteins or lipids causes oxidative stress; however adequate levels of ROS serve as signaling molecules that regulate physiological processes through redox signaling [91]. It was recently reported that a substantial but controlled increase in mitochondrial ROS levels takes place in BAT when mice are exposed to cold [31, 34]. This increase of ROS in BAT supports *in vivo* thermogenesis, since their depletion by the mitochondria-targeted antioxidant MitoQ or by NAC causes hypothermia in mice exposed to cold [31]. It has to be highlighted that there is no evidence of oxidative damage in BAT or increase in plasmatic reactive oxygen metabolites in mice exposed to cold [92], possibly due to the unique characteristics of the redox environment in BAT [33]. Importantly, we found that when mice were exposed to cold, TERRA levels increased in BAT but not in visceral WAT, fat depot that does not undergo an increase in mitochondrial ROS. Furthermore, exposure of mice to cold activates PKA signaling triggered by β-adrenergic stimulation of BAT [34]. We found evidence that PKA is required for induction of TERRA expression; therefore, it is possible that both ROS and the PKA signaling pathway may participate in the induction of TERRA in BAT when mice are facing a cold environment. In addition, a moderate but significant increase of TERRA levels was found in inguinal WAT depots, possibly due to the browning process that subcutaneous WAT undergoes in cold-exposed mice, an aspect that needs to be further investigated. The increase of TERRAs *in vivo* by physiological changes in ROS levels observed in BAT and in subcutaneous WAT may possibly be for telomere protection. It has been reported that

telomere dysfunction activates p53, which binds and represses the PGC-1α and PGC-1β promoter [93]. The PGC-1 family of co-activators plays a key role in the control of mitochondrial biogenesis and metabolic processes [94]. In BAT, PGC-1α controls key components of the adaptative thermogenic program. PGC-1α is rapidly induced upon cold exposure, activating UCP-1 expression. Thus, it is relevant to protect telomeres in response to the physiological increase of ROS by elevating TERRA, as shown in this study. Otherwise, damaged telomeres can become dysfunctional, triggering activation of p53, inhibition of PGC-1α and failure of UCP-1 expression, among other metabolic alterations, that will be detrimental for the thermogenic role of both brown and beige adipose cells, as well as for their metabolic homeostasis.

TERRA expression is dynamic. Their induction reverts shortly after the stressor (H_2O_2) is removed, reinforcing the idea that these lncRNAs may play a protective role. TERRA half-life has been estimated to be 2.2 h [4].}. We found that TERRA levels began to decrease within 2h of recovery from H_2O_2 exposure, result that is coherent with the reported TERRA half-life; thus, their downregulation would be associated with loss of active TERRA transcription. Interestingly, changes in the subtelomeric chromatin landscape acquired when cells were exposed to H_2O_2 for the first time were conserved, in a “transcriptional memory” kind of fashion. It has been recently reported that the release of promoter-proximal paused RNA pol II into elongation elicits the rapid expression of genes in response to heat stress [95]. Thus, the maintenance of H4Ac and RNA pol II paused at subtelomeric chromatin may allow cells rapidly to engaged RNA pol II into productive elongation, resulting in faster increased TERRA levels during a second oxidative challenge for them to become quickly available for protection of telomeres.

The chromatin landscape was modified at the subtelomeric domain to favor TERRA transcription when cells were exposed to H_2O_2. There was an increase in H3K9me3, a histone mark that forms a high affinity binding site for HP1 proteins [96]. In mammals, the three HP1 isoforms (HP1α, HP1β and HP1γ) present high sequence homology and identity, and yet they have different biochemical properties, different cellular localization patterns and divergent biological functions [96]. HP1α and HP1β associate predominantly with heterochromatin, whereas HP1γ is found both at heterochromatin and euchromatin, and can interact with RNA pol II [59] and nuclear actin [43], contributing to active transcription. Interestingly, HP1γ is the only member of the HP1 family that is not only present in the nucleus but also in the cytoplasm [43], making its biological role more complex. RIP assays for HP1α and HP1γ show that both isoforms interact with TERRA, and that

H_2O_2 exposure increases these TERRA interactions. It is tempting to hypothesize that an initial increase in TERRA transcription upon the onset of oxidative stress favors their interaction with HP1α/γ, and this would consequently favor their recruitment to subtelomeric domains in order to facilitate transcription. Therefore, enrichment of H3K9me3 and TERRA interaction with HP1s may favor an increased occupancy of HP1s at the subtelomeric region. In particular, HP1γ may favor the recruitment of RNA pol II and, along with the increased acetylation of histone H4, would consequently facilitate the transcription of TERRAs.

It has been reported that Nups can be targeted to active genes [97, 98]. Binding of nucleoplasmic Nups correlates with permissive transcription. For example, nucleoplasmic Nup98 preferentially binds to genes that are activated during the differentiation of human embryonic stem cells into neurons [99]. In contrast, binding of nuclear pore complex (NPC)-associated Nups correlates with repressive chromatin marks and low transcription [100, 101]. In spite of the acceptance that Nups participate in the control transcription as well as chromatin structure, little is known of how they bind to chromatin and exert these functions. Nup62 belongs to the peripheral/dynamic group of NPC proteins that can dynamically move on and off the pore. We found that HP1γ interacts with Nup62, therefore HP1γ may mediate Nup binding to chromatin, as we found by Re-ChIP assays at subtelomere 17p. It is likely that HP1γ may facilitate the recruitment of Nups to a large number of actively transcribed genes, a possibility that is under investigation. It has to be highlighted that neither Nup62 nor P-Ser5 RNA pol II nor nuclear actin co-immunoprecipitated with HP1α, in spite of the fact that the protein-interacting chromoshadow domain (CSD) of both HP1s show 87% sequence identity [102], reinforcing the notion that HP1γ is involved in the control of transcription at subtelomeres. HP1γ also interacts with actin, as we show in this study and a previous one [43]. Only recently has the concept of nuclear actin and its role in transcriptional control become consolidated. Nuclear actin interacts with RNA pol II [103, 104] and is present at the promoter and coding regions of constitutively expressed genes as shown by others and us [105]. We have recently shown that nuclear HP1γ and actin can form a complex at the promoter and coding regions of the actively transcribed *GAPDH* gene in myoblasts [43]. Now we show they are present at the subtelomeric domain, where TERRA transcription takes place. In summary, we propose a model in which H3K9me3 is necessary for stabilizing telomeres in response to oxidative stress, facilitating the binding of HP1α, as well as HP1γ. The former may contribute to telomeric heterochromatinization for stability. The latter has the capacity to interact not only with **RNA** pol II [59] and actin [43], but also with Nup62, as shown in this study for the first time. Thus, binding of HP1γ, actin and Nups,

accompanied by increased histone H4 acetylation, would facilitate accessibility of subtelomeric DNA to the transcriptional machinery when cells are exposed to an oxidative environment. Cells can conserve these changes in the subtelomeric chromatin landscape, in a “transcriptional memory” kind of fashion, possibly to allow them to induce TERRA levels faster during a second oxidative challenge in order to exert rapid protection of telomeres.

It has been demonstrated that ROS are required for the activation of signaling pathways in physiological conditions [91, 106]. PDGF and EGF increase ROS levels *via* NADPH oxidases in order to inhibit local tyrosine phosphatases [107] to allow proper phosphorylation of their tyrosine kinase receptors [108, 109]. It has also been reported that ROS can activate PKA by inducing the formation of disulfide bonds between its two regulatory subunits [69]. H_2O_2-dependent activation of PKA does not require an increase of intracellular cAMP levels [69], consistent with the finding that oxidants inhibit adenylate cyclase [71]. In our present study, we found that PKA activated either by H_2O_2 or by IBMX-Forskolin treatment of cells, participates in the control of TERRA transcription. Thus, this observation raises the possibility that other physiological situations in which PKA signaling is activated (i.e. by β-adrenergic stimulation of BAT upon cold exposure) may possibly lead to changes in TERRA transcription.

On the other hand, we have to keep in mind that cells are subjected to mechanical forces in their tissue microenvironment, and they have been shown to act in concert with chemical cues in order to properly regulate transcriptional programs in embryonic and adult tissues [110]. Mechanical stimuli from the environment are detected by changes in the conformation or the organization of proteins and cellular structures, including integrins, cadherins, phospholipases, stretch-sensitive ion channels, tyrosine kinase receptors and G protein-coupled receptors [77, 110]. These events can lead to the rapid activation of signaling cascades, such as FAK signaling at adhesion complexes [77, 111], and Src activation distally in the cytoplasm due to microtubule deformation [112, 113]. Alternatively, tensional forces can be transduced directly into the nucleus along the cytoskeleton, which is connected to the nuclear lamina by the LINC complex, leading to changes in cell architecture, gene expression and cellular functions [72]. It has been shown that mesenquimal stem cells (MSCs) simply grown on collagen-coated gels that mimic brain or muscle elasticity, not only exhibit the phenotypic characteristics of neuronal or muscle lineages, but also acquire a transcriptional profile inherent to each lineage [114]. Therefore, both soluble stimuli and the microenvironment’s stiffness impinge on the control of cellular functions. When HEK-293T cells were

grown on surfaces of varied stiffness, we observed significant changes in the cells' morphology, as shown due to cytoskeleton reorganization [48, 77], and we found that basal TERRA levels decreased as surface stiffness decreased. Importantly, cells grown on softer surfaces induced TERRA levels in response to a lower H_2O_2 concentration. Therefore, changes in the cytoskeleton impact not only on basal TERRA transcription, but also affect how cells regulate their expression in response to oxidative stress, in this case by increasing sensibility to an oxidative challenge. This is reasonable, since cells in tissues respond to lower H_2O_2 concentrations under physiological conditions [106]. ROS are known to tamper with the cytoskeleton, in particular, by affecting actin stress fiber formation [74]. In turn, we found that altering cytoskeleton dynamics either with H_2O_2, colcemid or paclitaxel treatment, caused an increase in TERRA levels. Lastly, C2C12 myoblast differentiation into myotubes also provided evidence that changes in the cytoskeleton influence TERRA levels; albeit it cannot be excluded that cell cycle exit and the onset of the differentiation process may also mediate control over TERRA transcription. Therefore, a delicate mecanotransduction mechanism may influence TERRA expression, where deviation from basal cytoskeleton organization, either due to disruption of microtubules (H_2O_2, colcemid), increased stability of microtubule fibers (paclitaxel) or reorganization of the cells' nucleoskeleton-cytoskeleton (hydrogel cultures, C2C12 myoblast differentiation), results in differential TERRA expression.

4. CONCLUSIONS

In the present study we show for the first time *in vitro* and *in vivo* that TERRA levels increase in response to an oxidative insult/stress (an excess of H_2O_2) or to oxidative eustress (physiological moderate increase in ROS), respectively, in order to protect telomeres, since they are particularly prone to suffer oxidative damage (**Figure 6**). PKA activation independent of cAMP levels, as well as changes in the cytoskeleton induced by ROS, mediate TERRA induction in response to oxidative stress. Changes in chromatin landscape at telomeres favor TERRA transcription. Subtelomeric increase of H3K9me3 promoted by H_2O_2 contributes to enrichment in HP1α, HP1γ, and consequently Nups and RNA Pol II, facilitating transcription at subtelomeres. Interestingly, this chromatin landscape is maintained as a sort of "cell memory", allowing cells faced with a second oxidative challenge to respond by rapidly increasing TERRA expression for telomere protection. Since TERRAs are highly expressed in many types of tumors and the tumor microenvironment is pro-oxidative, future studies will uncover the importance of TERRAs in this scenario.

Journal Pre-proof

Acknowledgments

This work was supported by grants from Agencia Nacional de Promoción Científica y Tecnológica to GPP (PICT2012-2612 and PICT2017-1692), Fundación René Barón and Fundación Williams. N.M.G. was a recipient of CONICET of a doctoral fellowship, and now has a postdoctoral fellowship. No competing interests declared.

Journal Pre-proof

REFERENCES

[1] T.R. Gingeras, Genome Res, 17 (2007) 682-690.
[2] C.A. Brosnan and O. Voinnet, Curr Opin Cell Biol, 21 (2009) 416-425.
[3] C.M. Azzalin, P. Reichenbach, L. Khoriauli, E. Giulotto and J. Lingner, Science, 318 (2007) 798-801.
[4] S. Schoeftner and M.A. Blasco, Nat Cell Biol, 10 (2008) 228-236.
[5] C.M. Azzalin and J. Lingner, Trends Cell Biol, 25 (2015) 29-36.
[6] A. Maicher, A. Lockhart and B. Luke, Biochim Biophys Acta, 1839 (2014) 387-394.
[7] E. Cusanelli, C.A. Romero and P. Chartrand, Mol Cell, 51 (2013) 780-91.
[8] B.O. Farnung, C.M. Brun, R. Arora, L.E. Lorenzi and C.M. Azzalin, PLoS One, 7 (2012) e35714.
[9] E. Cusanelli and P. Chartrand, Front Genet, 6 (2015) 143.
[10] Y. Negishi, H. Kawaji, A. Minoda and K. Usui, Biochem Biophys Res Commun, 467 (2015) 1052-1057.
[11] N. Arnoult, A. Van Beneden and A. Decottignies, Nat Struct Mol Biol, 19 (2012) 948-956.
[12] P.E. Thijssen, E.W. Tobi, J. Balog, S.G. Schouten, D. Kremer, F. El Bouazzaoui, P. Henneman, H. Putter, P. Eline Slagboom, B.T. Heijmans and S.M. van der Maarel, Epigenetics, 8 (2013) 512-521.
[13] S.G. Nergadze, B.O. Farnung, H. Wischnewski, L. Khoriauli, V. Vitelli, R. Chawla, E. Giulotto and C.M. Azzalin, Rna, 15 (2009) 2186-2194.
[14] M. Udugama, M.C. FT, F.L. Chan, M.C. Tang, H.A. Pickett, R.M. JD, L. Mayne, P. Collas, J.R. Mann and L.H. Wong, Nucleic Acids Res, 43 (2015) 10227-10237.
[15] M. Graf, D. Bonetti, A. Lockhart, K. Serhal, V. Kellner, A. Maicher, P. Jolivet, M.T. Teixeira and B. Luke, Cell, 170 (2017) 72-85 e14.
[16] R. Reig-Viader, M. Vila-Cejudo, V. Vitelli, R. Busca, M. Sabate, E. Giulotto, M.G. Caldes and A. Ruiz-Herrera, Biol Reprod, 90 (2014) 103.
[17] S. Yehezkel, A. Rebibo-Sabbah, Y. Segev, M. Tzukerman, R. Shaked, I. Huber, L. Gepstein, K. Skorecki and S. Selig, Epigenetics, 6 (2011) 63-75.
[18] R.M. Marion, K. Strati, H. Li, A. Tejera, S. Schoeftner, S. Ortega, M. Serrano and M.A. Blasco, Cell Stem Cell, 4 (2009) 141-154.
[19] Z. Deng, Z. Wang, C. Xiang, A. Molczan, V. Baubet, J. Conejo-Garcia, X. Xu, P.M. Lieberman and N. Dahmane, J Cell Sci, 125 (2012) 4383-4394.
[20] I. Lopez de Silanes, O. Grana, M.L. De Bonis, O. Dominguez, D.G. Pisano and M.A. Blasco, Nat Commun, 5 (2014) 4723.
[21] T. Finkel and N.J. Holbrook, Nature, 408 (2000) 239-247.
[22] M.T. Lin and M.F. Beal, Nature, 443 (2006) 787-795.
[23] U. Forstermann, Nat Clin Pract Cardiovasc Med, 5 (2008) 338-349.
[24] J.L. Rains and S.K. Jain, Free Radic Biol Med, 50 (2011) 567-575.
[25] S. Furukawa, T. Fujita, M. Shimabukuro, M. Iwaki, Y. Yamada, Y. Nakajima, O. Nakayama, M. Makishima, M. Matsuda and I. Shimomura, J Clin Invest, 114 (2004) 1752-1761.
[26] I.P. Tzanetakou, N.L. Katsilambros, A. Benetos, D.P. Mikhailidis and D.N. Perrea, Ageing Res Rev, 11 (2011) 220-229.
[27] M.J. Khandekar, P. Cohen and B.M. Spiegelman, Nat Rev Cancer, 11 (2011) 886-95.
[28] D. Hanahan and R.A. Weinberg, Cell, 144 (2011) 646-674.
[29] S.I. Grivennikov, F.R. Greten and M. Karin, Cell, 140 (2010) 883-899.
[30] P.D. Ray, B.W. Huang and Y. Tsuji, Cell Signal, 24 (2012) 981-990.

Journal Pre-proof

[31] E.T. Chouchani, L. Kazak, M.P. Jedrychowski, G.Z. Lu, B.K. Erickson, J. Szpyt, K.A. Pierce, D. Laznik-Bogoslavski, R. Vetrivelan, C.B. Clish, A.J. Robinson, S.P. Gygi and B.M. Spiegelman, Nature, 532 (2016) 112-116.
[32] G. Barja de Quiroga, M. Lopez-Torres, R. Perez-Campo, M. Abelenda, M. Paz Nava and M.L. Puerta, Biochem J, 277 (Pt 1) (1991) 289-292.
[33] R.J. Mailloux, C.N. Adjeitey, J.Y. Xuan and M.E. Harper, Faseb J, 26 (2012) 363-375.
[34] E.T. Chouchani, L. Kazak and B.M. Spiegelman, J Biol Chem, 292 (2017) 16810-16816.
[35] H. Sies, Redox Biol, 4 (2015) 180-183.
[36] R.M. Uranga, S. Katz and G.A. Salvador, J Biol Chem, 288 (2013) 19773-19784.
[37] D.B. Rhee, A. Ghosh, J. Lu, V.A. Bohr and Y. Liu, DNA Repair (Amst), 10 (2011) 34-44.
[38] S.F. Louis, B.J. Vermolen, Y. Garini, I.T. Young, A. Guffei, Z. Lichtensztejn, F. Kuttler, T.C. Chuang, S. Moshir, V. Mougey, A.Y. Chuang, P.D. Kerr, T. Fest, P. Boukamp and S. Mai, Proc Natl Acad Sci U S A, 102 (2005) 9613-9618.
[39] N. Takaha, A.L. Hawkins, C.A. Griffin, W.B. Isaacs and D.S. Coffey, Cancer Res, 62 (2002) 647-651.
[40] P.C. Fernandez, S.R. Frank, L. Wang, M. Schroeder, S. Liu, J. Greene, A. Cocito and B. Amati, Genes Dev, 17 (2003) 1115-1129.
[41] O. Vafa, M. Wade, S. Kern, M. Beeche, T.K. Pandita, G.M. Hampton and G.M. Wahl, Mol Cell, 9 (2002) 1031-1044.
[42] D. Jurk, C. Wilson, J.F. Passos, F. Oakley, C. Correia-Melo, L. Greaves, G. Saretzki, C. Fox, C. Lawless, R. Anderson, G. Hewitt, S.L. Pender, N. Fullard, G. Nelson, J. Mann, B. van de Sluis, D.A. Mann and T. von Zglinicki, Nat Commun, 2 (2014) 4172.
[43] N.L. Charo, N.M. Galigniana and G. Piwien-Pilipuk, Biochim Biophys Acta Mol Cell Res, 1865 (2018) 432-443.
[44] J. Toneatto, S. Guber, N.L. Charo, S. Susperreguy, J. Schwartz, M.D. Galigniana and G. Piwien-Pilipuk, J Cell Sci, 126 (2013) 5357-5368.
[45] S. Susperreguy, L.P. Prendes, M.A. Desbats, N.L. Charo, K. Brown, O.A. MacDougald, T. Kerppola, J. Schwartz and G. Piwien-Pilipuk, Exp Cell Res, 317 (2011) 706-723.
[46] Z. Deng, Z. Wang, N. Stong, R. Plasschaert, A. Moczan, H.S. Chen, S. Hu, P. Wikramasinghe, R.V. Davuluri, M.S. Bartolomei, H. Riethman and P.M. Lieberman, Embo J, 31 (2012) 4165-4178.
[47] L.A. Selth, P. Close and J.Q. Svejstrup, Methods Mol Biol, 791 (2011) 253-264.
[48] L. Przybyla, J.N. Lakins, R. Sunyer, X. Trepat and V.M. Weaver, Methods, 94 (2016) 101-113.
[49] C.A. Worthen, L. Rittie and G.J. Fisher, Methods Mol Biol, 1627 (2017) 245-51.
[50] L. Crabbe, A.J. Cesare, J.M. Kasuboski, J.A. Fitzpatrick and J. Karlseder, Cell Rep, 2 (2012) 1521-1529.
[51] G. Hewitt, D. Jurk, F.D. Marques, C. Correia-Melo, T. Hardy, A. Gackowska, R. Anderson, M. Taschuk, J. Mann and J.F. Passos, Nat Commun, 3 (2012) 708.
[52] O. Moujaber, H. Mahboubi, M. Kodiha, M. Bouttier, K. Bednarz, R. Bakshi, J. White, L. Larose, I. Colmegna and U. Stochaj, Biochim Biophys Acta Mol Cell Res, 1864 (2017) 475-486.
[53] S. Waris, M.C. Wilce and J.A. Wilce, Int J Mol Sci, 15 (2014) 23377-23388.
[54] R. Benetti, M. Garcia-Cao and M.A. Blasco, Nat Genet, 39 (2007) 243-250.
[55] M.A. Blasco, Nat Rev Genet, 8 (2007) 299-309.
[56] A.J. Bannister, P. Zegerman, J.F. Partridge, E.A. Miska, J.O. Thomas, R.C. Allshire and T. Kouzarides, Nature, 410 (2001) 120-124.
[57] M. Lachner, D. O'Carroll, S. Rea, K. Mechtler and T. Jenuwein, Nature, 410 (2001) 116-120.
[58] J. Nakayama, J.C. Rice, B.D. Strahl, C.D. Allis and S.I. Grewal, Science, 292 (2001) 110-113.
[59] C.R. Vakoc, S.A. Mandat, B.A. Olenchock and G.A. Blobel, Mol Cell, 19 (2005) 381-391.
[60] G. Lomberk, D. Bensi, M.E. Fernandez-Zapico and R. Urrutia, Nat Cell Biol, 8 (2006) 407-415.

Journal Pre-proof

[61] P. Pascual-Garcia and M. Capelson, Curr Opin Genet Dev, 25 (2014) 110-117.
[62] A. Ibarra and M.W. Hetzer, Genes Dev, 29 (2015) 337-349.
[63] L.I. Davis and G. Blobel, Proc Natl Acad Sci U S A, 84 (1987) 7552-7556.
[64] R.I. Lopez-Soler, R.D. Moir, T.P. Spann, R. Stick and R.D. Goldman, J Cell Biol, 154 (2001) 61-70.
[65] K. Hiragami and R. Festenstein, Cell Mol Life Sci, 62 (2005) 2711-2726.
[66] Z. Deng, J. Norseen, A. Wiedmer, H. Riethman and P.M. Lieberman, Mol Cell, 35 (2009) 403-413.
[67] B. Enjalbert, A. Nantel and M. Whiteway, Mol Biol Cell, 14 (2003) 1460-1467.
[68] M. Gialitakis, P. Arampatzi, T. Makatounakis and J. Papamatheakis, Mol Cell Biol, 30 (2010) 2046-2056.
[69] J.P. Brennan, S.C. Bardswell, J.R. Burgoyne, W. Fuller, E. Schroder, R. Wait, S. Begum, J.C. Kentish and P. Eaton, J Biol Chem, 281 (2006) 21827-21836.
[70] S. Persad, V. Panagia and N.S. Dhalla, Mol Cell Biochem, 186 (1998) 99-106.
[71] G.I. Drummond, Arch Biochem Biophys, 211 (1981) 30-38.
[72] G.R. Fedorchak, A. Kaminski and J. Lammerding, Prog Biophys Mol Biol, 115 (2014) 76-92.
[73] S. Osmanagic-Myers, T. Dechat and R. Foisner, Genes Dev, 29 (2015) 225-237.
[74] T. Fiaschi, G. Cozzi, G. Raugei, L. Formigli, G. Ramponi and P. Chiarugi, J Biol Chem, 281 (2006) 22983-22991.
[75] T. Enomoto, Cell Struct Funct, 21 (1996) 317-326.
[76] R.B. Vallee and C.A. Collins, Methods Enzymol, 134 (1986) 116-127.
[77] C.C. DuFort, M.J. Paszek and V.M. Weaver, Nat Rev Mol Cell Biol, 12 (2011) 308-319.
[78] M. Berendse, M.D. Grounds and C.M. Lloyd, Exp Cell Res, 291 (2003) 435-450.
[79] S. Burattini, P. Ferri, M. Battistelli, R. Curci, F. Luchetti and E. Falcieri, Eur J Histochem, 48 (2004) 223-233.
[80] J. White, M.V. Barro, H.P. Makarenkova, J.W. Sanger and J.M. Sanger, Anat Rec (Hoboken), 297 (2014) 1571-1584.
[81] X. Xu, M. Guo, N. Zhang and S. Ye, Am J Physiol Cell Physiol, 314 (2018) C712-720.
[82] S.S. Sabharwal and P.T. Schumacker, Nat Rev Cancer, 14 (2014) 709-721.
[83] I.B. Slimen, T. Najar, A. Ghram, H. Dabbebi, M. Ben Mrad and M. Abdrabbah, Int J Hyperthermia, 30 (2014) 513-523.
[84] D.E. Handy and J. Loscalzo, Free Radic Biol Med, 109 (2017) 114-124.
[85] F. Singh, A.L. Charles, A.I. Schlagowski, J. Bouitbir, A. Bonifacio, F. Piquard, S. Krahenbuhl, B. Geny and J. Zoll, Biochim Biophys Acta, 1853 (2015) 1574-1585.
[86] A. Tchirkov and P.M. Lansdorp, Hum Mol Genet, 12 (2003) 227-232.
[87] L. Liu, J.R. Trimarchi, P. Navarro, M.A. Blasco and D.L. Keefe, J Biol Chem, 278 (2003) 31998-32004.
[88] S. Kawanishi and S. Oikawa, Ann N Y Acad Sci, 1019 (2004) 278-284.
[89] A.T. Ludlow, E.E. Spangenburg, E.R. Chin, W.H. Cheng and S.M. Roth, J Gerontol A Biol Sci Med Sci, 69 (2014) 821-830.
[90] R. Arora, C.M. Brun and C.M. Azzalin, RNA, 18 (2012) 684-693.
[91] M. Schieber and N.S. Chandel, Curr Biol, 24 (2014) R453-462.
[92] A. Stier, P. Bize, C. Habold, F. Bouillaud, S. Massemin and F. Criscuolo, J Exp Biol, 217 (2014) 624-630.
[93] E. Sahin, S. Colla, M. Liesa, J. Moslehi, F.L. Muller, M. Guo, M. Cooper, D. Kotton, A.J. Fabian, C. Walkey, R.S. Maser, G. Tonon, F. Foerster, R. Xiong, Y.A. Wang, S.A. Shukla, M. Jaskelioff, E.S. Martin, T.P. Heffernan, A. Protopopov, E. Ivanova, J.E. Mahoney, M. Kost-Alimova, S.R. Perry, R. Bronson, R. Liao, R. Mulligan, O.S. Shirihai, L. Chin and R.A. DePinho, Nature, 470 (2011) 359-365.

Journal Pre-proof

[94] J. Lin, C. Handschin and B.M. Spiegelman, Cell Metab, 1 (2005) 361-370.
[95] A. Vihervaara, D.B. Mahat, M.J. Guertin, T. Chu, C.G. Danko, J.T. Lis and L. Sistonen, Nat Commun, 8 (2017) 255.
[96] G. Nishibuchi and J. Nakayama, J Biochem, 156 (2014) 11-20.
[97] G. Rabut, V. Doye and J. Ellenberg, Nat Cell Biol, 6 (2004) 1114-1121.
[98] E.R. Griffis, B. Craige, C. Dimaano, K.S. Ullman and M.A. Powers, Mol Biol Cell, 15 (2004) 1991-2002.
[99] Y. Liang, T.M. Franks, M.C. Marchetto, F.H. Gage and M.W. Hetzer, PLoS Genet, 9 (2013) e1003308.
[100] M. Capelson, Y. Liang, R. Schulte, W. Mair, U. Wagner and M.W. Hetzer, Cell, 140 (2010) 372-383.
[101] B. Kalverda, H. Pickersgill, V.V. Shloma and M. Fornerod, Cell, 140 (2010) 360-371.
[102] D. Canzio, A. Larson and G.J. Narlikar, Trends Cell Biol, 24 (2014) 377-386.
[103] W.A. Hofmann, L. Stojiljkovic, B. Fuchsova, G.M. Vargas, E. Mavrommatis, V. Philimonenko, K. Kysela, J.A. Goodrich, J.L. Lessard, T.J. Hope, P. Hozak and P. de Lanerolle, Nat Cell Biol, 6 (2004) 1094-1101.
[104] A. Kukalev, Y. Nord, C. Palmberg, T. Bergman and P. Percipalle, Nat Struct Mol Biol, 12 (2005) 238-244.
[105] A. Obrdlik, A. Kukalev, E. Louvet, A.K. Farrants, L. Caputo and P. Percipalle, Mol Cell Biol, 28 (2008) 6342-6357.
[106] H. Sies, Redox Biol, 11 (2017) 613-619.
[107] T.C. Meng, T. Fukada and N.K. Tonks, Mol Cell, 9 (2002) 387-399.
[108] M. Sundaresan, Z.X. Yu, V.J. Ferrans, K. Irani and T. Finkel, Science, 270 (1995) 296-299.
[109] Y.S. Bae, S.W. Kang, M.S. Seo, I.C. Baines, E. Tekle, P.B. Chock and S.G. Rhee, J Biol Chem, 272 (1997) 217-221.
[110] A. Mammoto, T. Mammoto and D.E. Ingber, J Cell Sci, 125 (2012) 3061-3073.
[111] M.K.L. Han and J. de Rooij, Trends Cell Biol, 26 (2016) 612-623.
[112] Y. Wang, E.L. Botvinick, Y. Zhao, M.W. Berns, S. Usami, R.Y. Tsien and S. Chien, Nature, 434 (2005) 1040-1045.
[113] S. Na, O. Collin, F. Chowdhury, B. Tay, M. Ouyang, Y. Wang and N. Wang, Proc Natl Acad Sci U S A, 105 (2008) 6626-6631.
[114] A.J. Engler, S. Sen, H.L. Sweeney and D.E. Discher, Cell, 126 (2006) 677-689.

Journal Pre-proof

Figure legends

Figure 1: TERRAs are induced by oxidative stress in HEK-293T cells. (**A**) Representative confocal images of telomeric marker TRF1 (green) and DNA damage marker P-Ser139 H2AX (γH2AX, red) in HEK-293T cells. Nuclei were stained with DAPI (blue). Scale bar: 5μm. (**B**) Total number and fluorescence intensities of γH2AX foci were measured in at least 30 nuclei, and graphed as mean±SD. *P-values* were calculated by two-tailed Student's *t*-test. (**C**) Percentage of TAFs per nucleus corresponding to TRF1 co-localizing with γH2AX in cells incubated in the absence or the presence of H_2O_2. Data are mean±SD of at least 30 nuclei. *P-values* were calculated by two-tailed Student's *t*-test. (**D**) qPCR of TERRAs after 4h exposure to the indicated concentrations of H_2O_2. The ΔΔCt method was used relative to GAPDH and the control group in order to calculate relative TERRA expression by qPCR. Bar graphs represent the mean±SD from 3 independent experiments. *P-values* (one-way ANOVA with *post hoc* Tukey's test) are indicated for each TERRA relative to their Control: * $P<0.05$; ** $P<0.01$; n.s.: not significant. (**E**) Cells were treated with 500μM H_2O_2 for the indicated time points and TERRA expression was evaluated by end-point PCR. Representative agarose gels are shown here from 5 independent experiments. (**F**) Confocal images of cytoplasmic stress granule formation by staining TIAR (green; panel II, see arrows), which is blocked by co-incubation with NAC (panel IV). (**G**) End-point PCR and (**H**) qPCR of TERRA from samples of cells incubated 4h in the absence or the presence of 500μM H_2O_2 with or without 5mM NAC. The ΔΔCt method was used as described in D. Statistical analysis was performed using a two-tailed Student's *t*-test (Control vs. H_2O_2; NAC vs. NAC+H_2O_2). n.s.: not significant. (**I**) qPCR of TERRAs in three different fat depots obtained from male C57BL/6J mice kept at room temperature (RT) or at 4°C for 4h. Data are mean±SD of five mice replicates. Analysis was performed as in H.

Figure 2: H_2O_2 exposure changes subtelomeric chromatin landscape and favors TERRA interaction with HP1γ. (**A**) ChIP was performed using antibodies for H3K9me3, H4Ac, HP1α, HP1γ, P-Ser5 RNApol II, mAb 414 that recognizes Nups or non-immune IgG, as described in Materials and Methods. Representative agarose gels of PCRs using primer pairs for the 17p subtelomeric region are shown. Results are representative of 3 independent experiments. (**B**) HP1γ or HP1α immunoprecipitated from nuclear fractions of HEK-293T cells were resolved by SDS-PAGE and analyzed by immunoblotting with the indicated antibodies. NI: non-immune antibody. Results are representative of 3 independent experiments. (**C**) HP1γ was immunoprecipitated form nuclear fractions of cells incubated in the absence or the presence of H_2O_2, and protein complexes were

analyzed by WB (n=3). (**D**) For re-ChIP assays, the beads from the first IP with anti-HP1γ were washed, eluted and subjected to a second IP with mAb 414, anti- actin or non-immune IgG. Representative results of PCRs with primer pairs for the 17p subtelomeric region are shown. (**E**) Representative agarose gels of end-point PCRs for 17p TERRAs present in samples obtained by subcellular fractionation of HEK-293T cells exposed or not to H_2O_2. The graph shows densitometric analysis of band intensities relative to GAPDH and control cells. Data represent the mean±SD from 4 independent experiments. Statistical analysis was performed using a two-tailed Student's *t*-test (Control vs. H_2O_2). n.s.: not significant; AU: arbitrary units. (**F**) For RIP assays, HP1γ or HP1α were immunoprecipitated and RNA was isolated and analyzed as indicated in Materials and Methods. Bottom numbers indicate band intensities relative to the control of this agarose gel that is representative of 3 independent experiments. Input: total RNA.

Figure 3: TERRA induction is dynamic. (**A**) HEK-293T cells were incubated 4h with 500μM H_2O_2, then washed to eliminate residual H_2O_2 and fresh medium was added to harvest cells at the indicated time points. Agarose gels are representative of 3 independent experiments. (**B**) Densitometric analysis of TERRA band intensities from A relative to GAPDH and control cells. Data represent the mean±SD. Significant differences (one-way ANOVA with *post hoc* Tukey's test) to respective controls are indicated by * for $P<0.05$ and ** for $P<0.01$. AU: arbitrary units. (**C**) Schematic representation of experimental design. Below, representative agarose gels from 3 independent experiments are shown. (**D**) Densitometric analysis of C performed as explained in B. * $P<0.05$; ** $P<0.01$; *** $P<0.001$. AU: arbitrary units. (**E**) ChIPs performed following the experimental design in C. Representative agarose gels from 3 independent experiments are shown. Rec 24h: cells allowed to recover 24h in fresh culture medium; Rec+15'H_2O_2: cells recovered 24h and then treated 15min with 500μM H_2O_2; Input: total genomic DNA.

Figure 4: PKA signaling controls TERRA induction by oxidative stress. (**A**) HEK-293T cells were incubated with H_2O_2 in the absence or the presence of H89 for the indicated periods of time. Cells were harvested and analyzed by WB with the indicated antibodies. (**B**) Cells were incubated with IBMX+Forskolin in the absence or the presence of H89 and samples analyzed as in A. (**C**) HEK293T cells were incubated with IBMX+Forskolin or H_2O_2 in the absence or the presence of H89, RNA was isolated and TERRAs measured by qPCR. The ΔΔCt method was used relative to GAPDH and the control group in order to calculate relative TERRA expression. Bar graphs represent the mean±SD

from 3 independent experiments. *P-values* (one-way ANOVA with *post hoc* Tukey's test) are indicated for each TERRA relative to their Control: * *P*<0.05; ** *P*<0.01; *** *P*<0.001; n.s.: not significant. (**D**) qPCR of individual TERRAs from cells incubated with H_2O_2 in the absence or the presence of PKI. Analysis was performed as described in C. Concentrations used: 500µM H_2O_2; 52µM IBMX + 30µM Forskolin; 20µM H89; 0.5µM PKI.

Figure 5: Changes in the dynamic organization of microtubules may regulate TERRA transcription. (**A-B**) Cells grown on coverslips were treated 4h with 500µM H_2O_2 or 2h with 0.6 µg/ml colcemid, and then fixed and stained with anti-α-tubulin (green) or anti-TIAR (red). Representative confocal images are shown. Arrows indicate cytoplasmic α-tubulin aggregates (panels b and c) or stress granules (panel e). Scale bars: 10µm. (**C**) Cells were incubated with colcemid for the indicated periods of time. Cells were harvested, RNA isolated and TERRA evaluated by end-point PCR. Representative agarose gels from 3 independent experiments are shown. (**D**) Cells were incubated with H_2O_2 and/or paclitaxel as indicated, they were harvested, RNA isolated and TERRA evaluated by end-point PCR. Representative agarose gels from 3 independent experiments. (**E**) Phase contrast microscopy images of HEK-293T cells grown for 24h on hydrogels of increasing surface stiffness (elastic moduli (E) of 1.05kPa or 60kPa) or with no gel directly on the plastic cell culture dish. Images were taken with 40X magnification in 3 independent experiments. (**F**) qPCR of individual TERRAs from cells grown on surfaces of different stiffness as indicated in E. Data represent the mean±SD of 3 independent experiments. Significant differences (one-way ANOVA with *post hoc* Tukey's test) to respective "No gel" controls are indicated by * (* *P*<0.05; ** *P*<0.01; *** *P*<0.001), and between soft and stiff gels by # (# *P*<0.05; ## *P*<0.01; ### *P*<0.001). (**G**) Cells grown on hydrogels of E=60kPa or directly on plastic cell culture dishes (No gel) were treated 4h with H_2O_2 at the indicated concentrations. TERRA levels were measured by qPCR. Data represent the mean±SD of 3 independent experiments. *P-values* were calculated by one-way ANOVA with *post hoc* Tukey's test, and are indicated for each TERRA relative to their Control: * *P*<0.05; ** *P*<0.01; n.s.: not significant. (**H**) Representative confocal images of α-tubulin or phalloidin (both green) showing microtubule (panel a vs. b) and actin microfilament (panel c vs. d) rearrangements of C2C12 myoblasts 4 days post-induction of differentiation (n=3). Nuclei were stained with DAPI (blue). Scale bars: 5µm. (**I**) TERRAs were measured by qPCR in C2C12 myoblasts and myotubes. Data represent the mean±SD (n=3). Statistical analysis was performed using a two-tailed Student's *t*-test (* *P*<0.05; ** *P*<0.01; *** *P*<0.001; n.s.: not significant).

Figure 6: Control of TERRA expression upon oxidative stress. H_2O_2 increases TERRA levels mainly in the cell nucleus by inducing changes in the chromatin landscape of subtelomeres. H3K93Me and acetylation of histone H4 are increased, along with binding of HP1α and HP1γ, the latter favoring the recruitment of P-Ser5 RNA pol II, Nup62 and possibly actin, in order to facilitate transcription at subtelomeres when cells are exposed to oxidative stress. This chromatin landscape is conserved after the initial H_2O_2 exposure, allowing cells faced with a second oxidative challenge to respond by rapidly increasing TERRA expression for telomere protection. PKA activation independent of cAMP levels, as well as changes in the cytoskeleton induced by ROS, control TERRA induction in response to oxidative stress.

Journal Pre-proof

Research Highlights

- Oxidative stress induces the expression of TERRA (telomeric repeat-containing RNA).
- Increased ROS in brown adipose tissue induces TERRA expression *in vivo*.
- The subtelomeric chromatin landscape changes to favor TERRA transcription.
- TERRAs interact with HP1γ.
- PKA signaling and changes in cytoskeleton dynamics regulate TERRA induction.

Journal Pre-proof

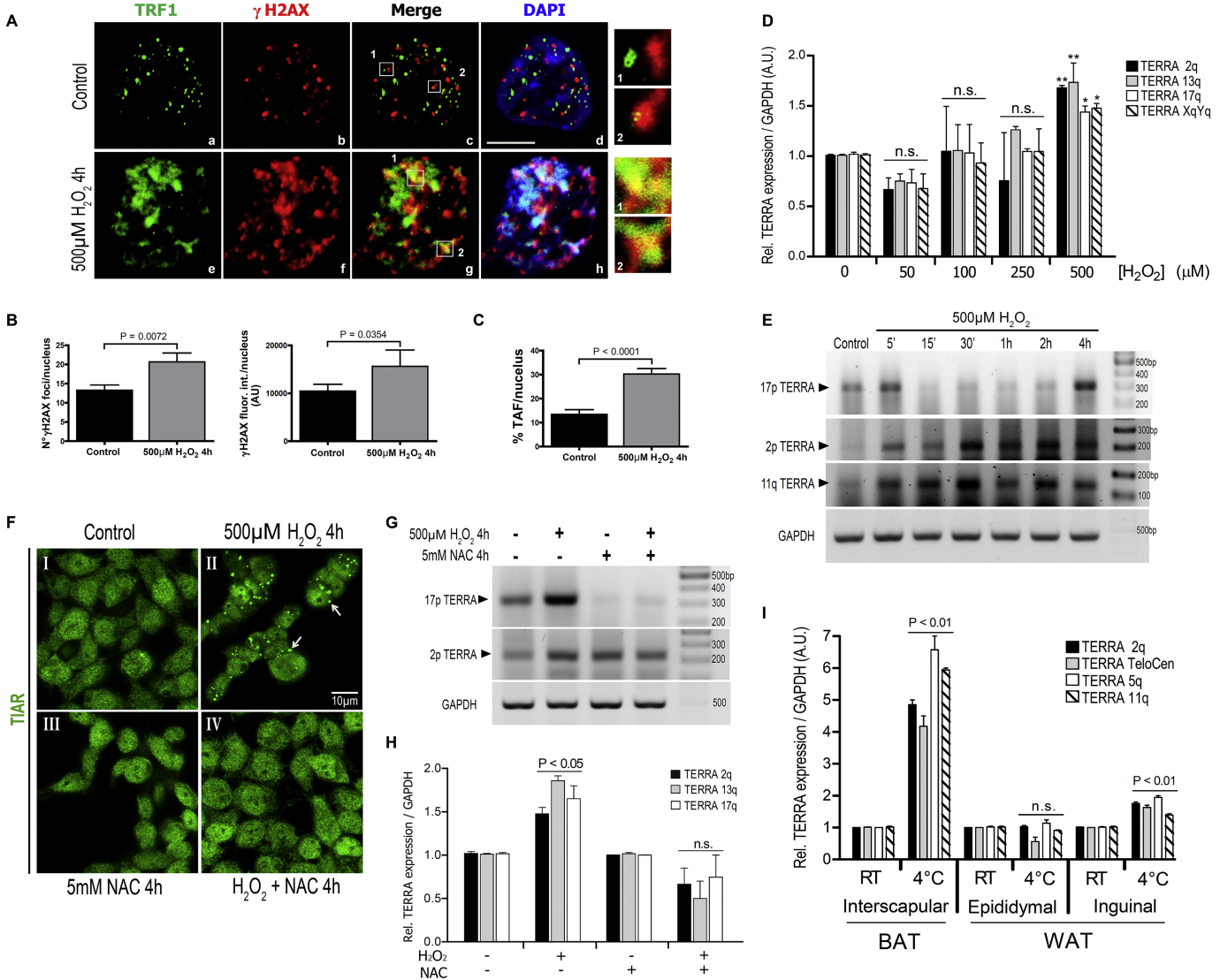
A
TRF1
γ H2AX
Merge
DAPI
Control
500μM H2O2 4h
a
b
c
d
e
f
g
h
B
P = 0.0072
N° γH2AX foci/nucleus
Control
500μM H2O2 4h
P = 0.0354
γH2AX fluor. int./nucleus (AU)
C
P < 0.0001
% TAF/nucleus
D
Rel. TERRA expression / GAPDH (A.U.)
TERRA 2q
TERRA 13q
TERRA 17q
TERRA XqYq
n.s.
[H2O2] (μM)
E
500μM H2O2
Control
5'
15'
30'
1h
2h
4h
17p TERRA
2p TERRA
11q TERRA
GAPDH
F
Control
500μM H2O2 4h
TIAR
10μm
5mM NAC 4h
H2O2 + NAC 4h
G
500μM H2O2 4h
5mM NAC 4h
17p TERRA
2p TERRA
GAPDH
H
P < 0.05
Rel. TERRA expression / GAPDH
TERRA 2q
TERRA 13q
TERRA 17q
n.s.
H2O2
NAC
I
P < 0.01
Rel. TERRA expression / GAPDH (A.U.)
TERRA 2q
TERRA TeloCen
TERRA 5q
TERRA 11q
RT
4°C
Interscapular
Epididymal
Inguinal
BAT
WAT

Figure 1

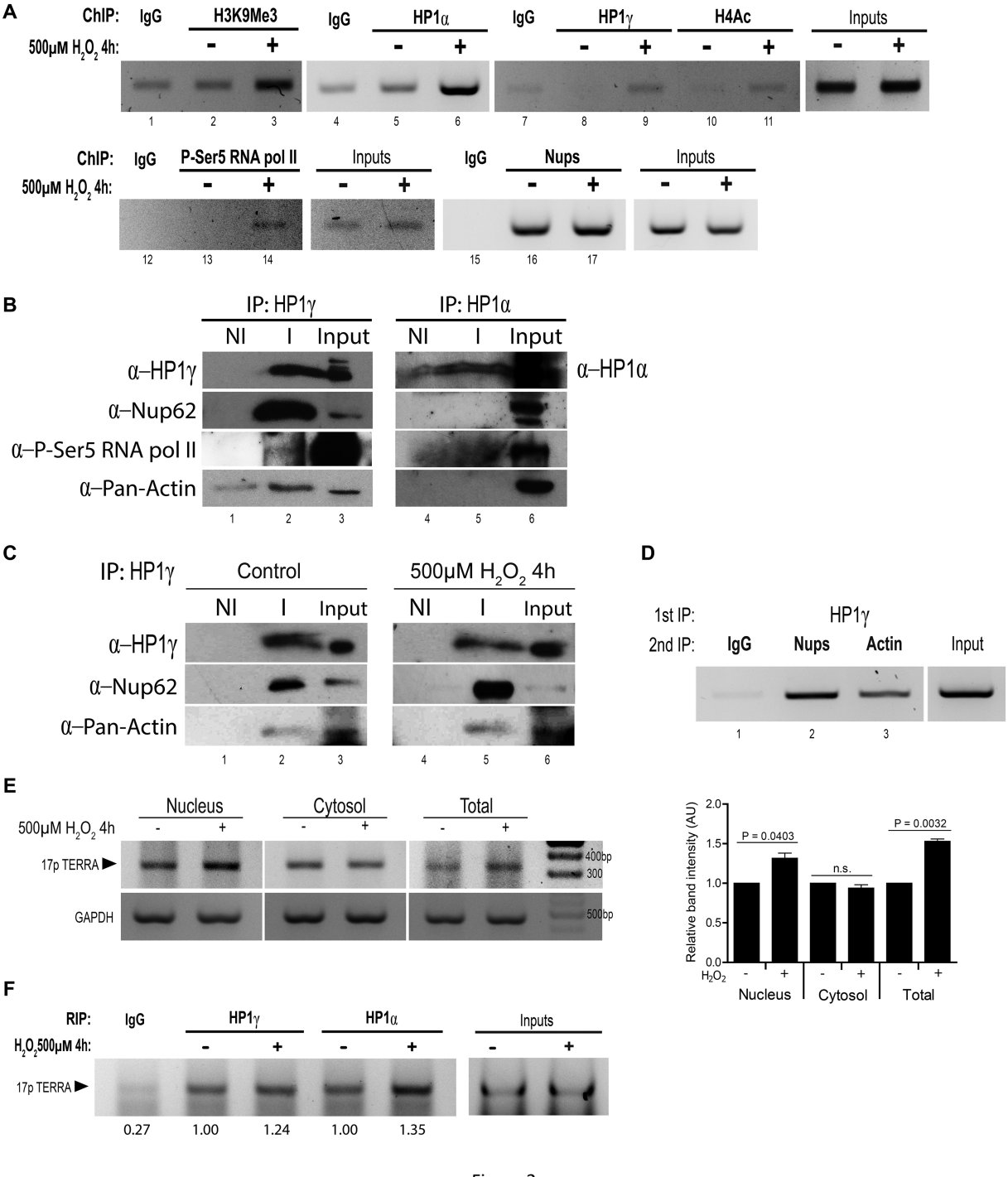
A
ChIP: IgG H3K9Me3 IgG HP1α IgG HP1γ H4Ac Inputs
500μM H2O2 4h: - + - + - + - + - +
1 2 3 4 5 6 7 8 9 10 11
ChIP: IgG P-Ser5 RNA pol II Inputs IgG Nups Inputs
500μM H2O2 4h: - + - + - + - +
12 13 14 15 16 17
B
IP: HP1γ IP: HP1α
NI I Input NI I Input
α–HP1γ
α–Nup62
α–P-Ser5 RNA pol II
α–Pan-Actin
α–HP1α
1 2 3 4 5 6
C
IP: HP1γ Control 500μM H2O2 4h
NI I Input NI I Input
α–HP1γ
α–Nup62
α–Pan-Actin
1 2 3 4 5 6
D
1st IP: HP1γ
2nd IP: IgG Nups Actin Input
1 2 3
E
Nucleus Cytosol Total
500μM H2O2 4h - + - + - +
17p TERRA
GAPDH
400bp
300
500bp
Relative band intensity (AU)
2.0
1.5
1.0
0.5
0.0
P = 0.0403
n.s.
P = 0.0032
H2O2 - + - + - +
Nucleus Cytosol Total
F
RIP: IgG HP1γ HP1α Inputs
H2O2 500μM 4h: - + - + - +
17p TERRA
0.27 1.00 1.24 1.00 1.35

Figure 2

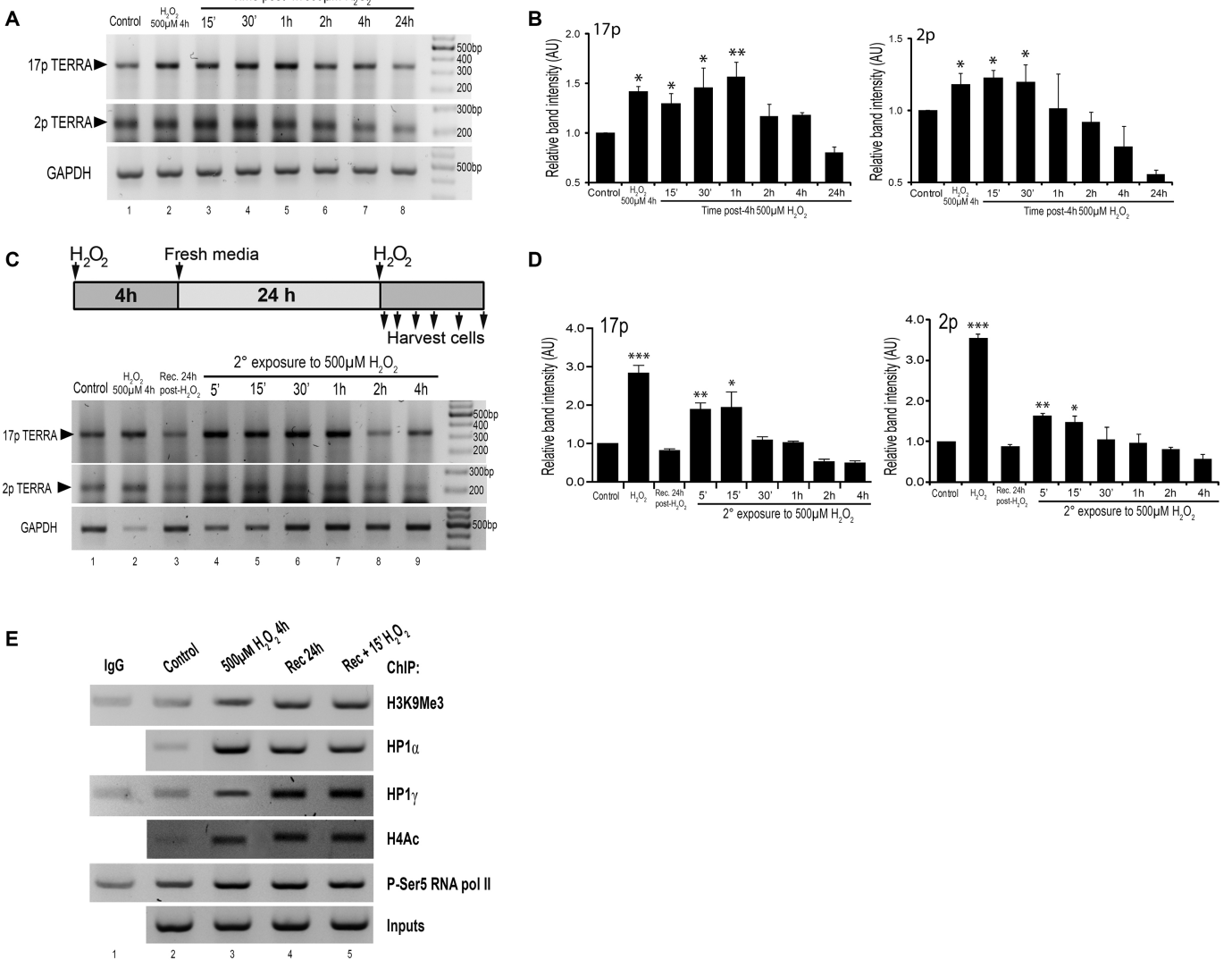
A
Time post-4h 500μM H_2O_2
Control
H_2O_2 500μM 4h
15'
30'
1h
2h
4h
24h
17p TERRA
2p TERRA
GAPDH
500bp
400
300
200
300bp
200
500bp
1 2 3 4 5 6 7 8
B
17p
2p
Relative band intensity (AU)
Time post-4h 500μM H_2O_2
C
H_2O_2
Fresh media
H_2O_2
4h
24 h
Harvest cells
2° exposure to 500μM H_2O_2
Rec. 24h post-H_2O_2
5'
17p TERRA
2p TERRA
GAPDH
1 2 3 4 5 6 7 8 9
D
17p
2p
Relative band intensity (AU)
Control
H_2O_2
Rec. 24h post-H_2O_2
2° exposure to 500μM H_2O_2
E
IgG
Control
500μM H_2O_2 4h
Rec 24h
Rec + 15' H_2O_2
ChIP:
H3K9Me3
HP1α
HP1γ
H4Ac
P-Ser5 RNA pol II
Inputs
1 2 3 4 5

Figure 3

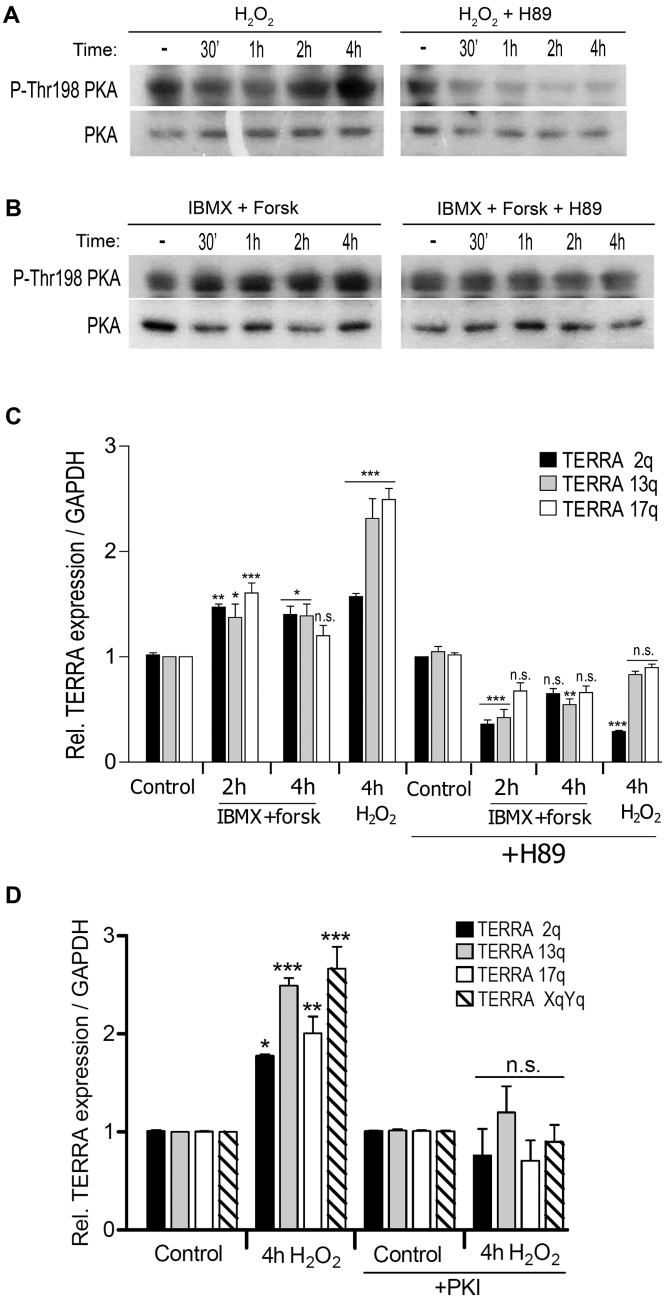
A
H2O2
H2O2 + H89
Time:
-
30'
1h
2h
4h
P-Thr198 PKA
PKA
B
IBMX + Forsk
IBMX + Forsk + H89
C
Rel. TERRA expression / GAPDH
TERRA 2q
TERRA 13q
TERRA 17q
n.s.
Control
2h
4h
IBMX+forsk
4h H2O2
+H89
D
TERRA XqYq
+PKI

Figure 4

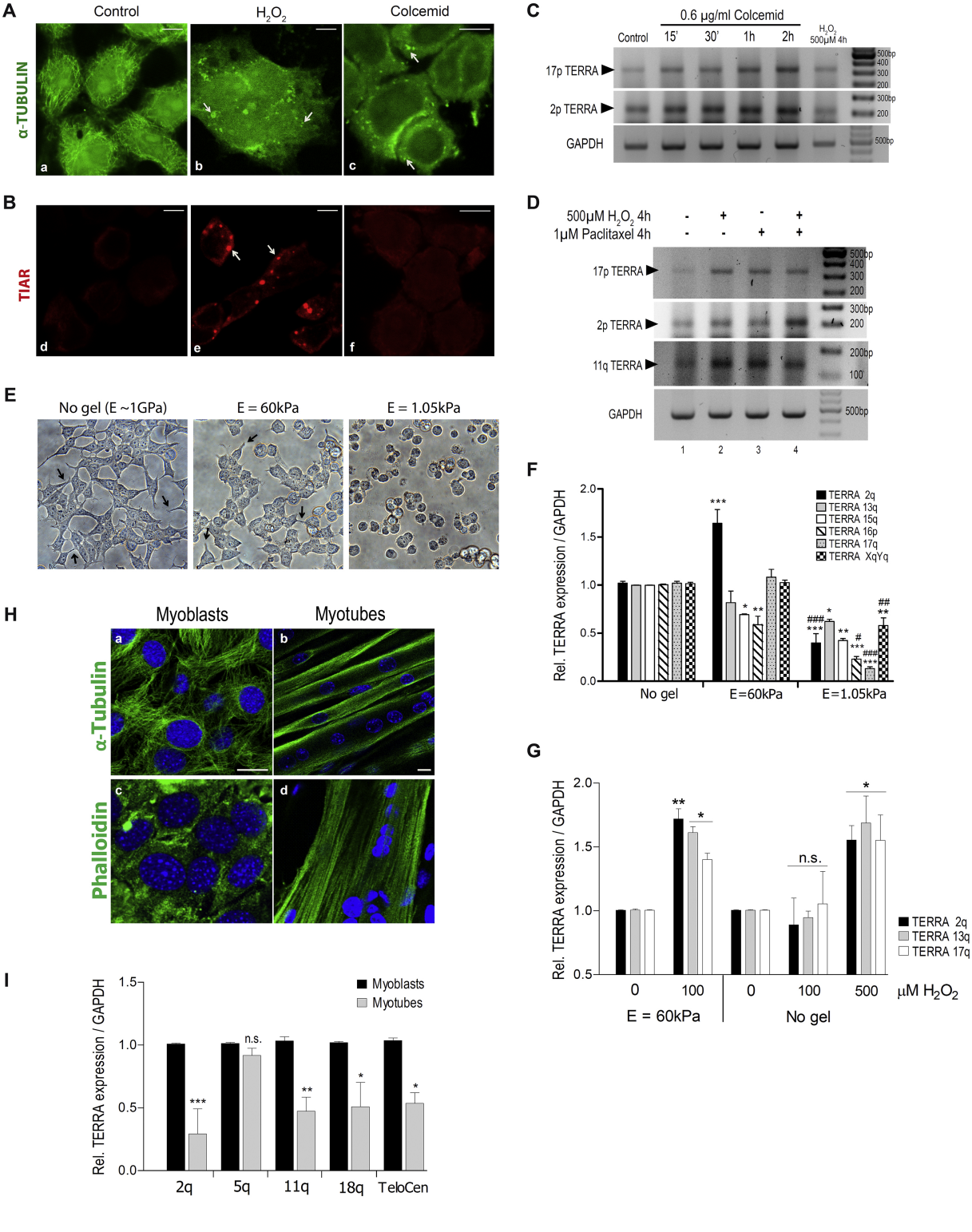
A
Control
H2O2
Colcemid
α-TUBULIN
a
b
c
B
TIAR
d
e
f
C
0.6 µg/ml Colcemid
Control
15'
30'
1h
2h
H2O2 500µM 4h
17p TERRA
2p TERRA
GAPDH
500bp
400
300
200
300bp
200
500bp
D
500µM H2O2 4h
1µM Paclitaxel 4h
17p TERRA
2p TERRA
11q TERRA
GAPDH
500bp
400
300
200
300bp
200
200bp
100
500bp
1
2
3
4
E
No gel (E ~1GPa)
E = 60kPa
E = 1.05kPa
F
Rel. TERRA expression / GAPDH
2.0
1.5
1.0
0.5
0.0
TERRA 2q
TERRA 13q
TERRA 15q
TERRA 16p
TERRA 17q
TERRA XqYq
No gel
E=60kPa
E=1.05kPa
G
Rel. TERRA expression / GAPDH
2.0
1.5
1.0
0.5
n.s.
TERRA 2q
TERRA 13q
TERRA 17q
0
100
0
100
500
µM H2O2
E = 60kPa
No gel
H
Myoblasts
Myotubes
α-Tubulin
Phalloidin
a
b
c
d
I
Rel. TERRA expression / GAPDH
1.5
1.0
0.5
0.0
n.s.
Myoblasts
Myotubes
2q
5q
11q
18q
TeloCen

Figure 5

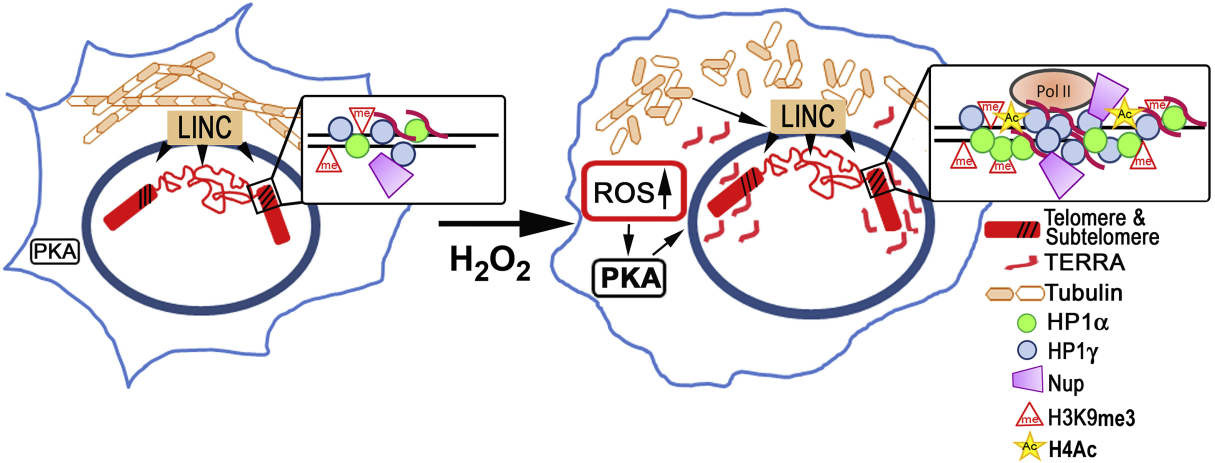
LINC
PKA
me
me
H_2O_2
ROS
PKA
LINC
Pol II
me
Ac
me
Ac
me
me
me
Telomere &
Subtelomere
TERRA
Tubulin
HP1α
HP1γ
Nup
H3K9me3
H4Ac

Figure 6

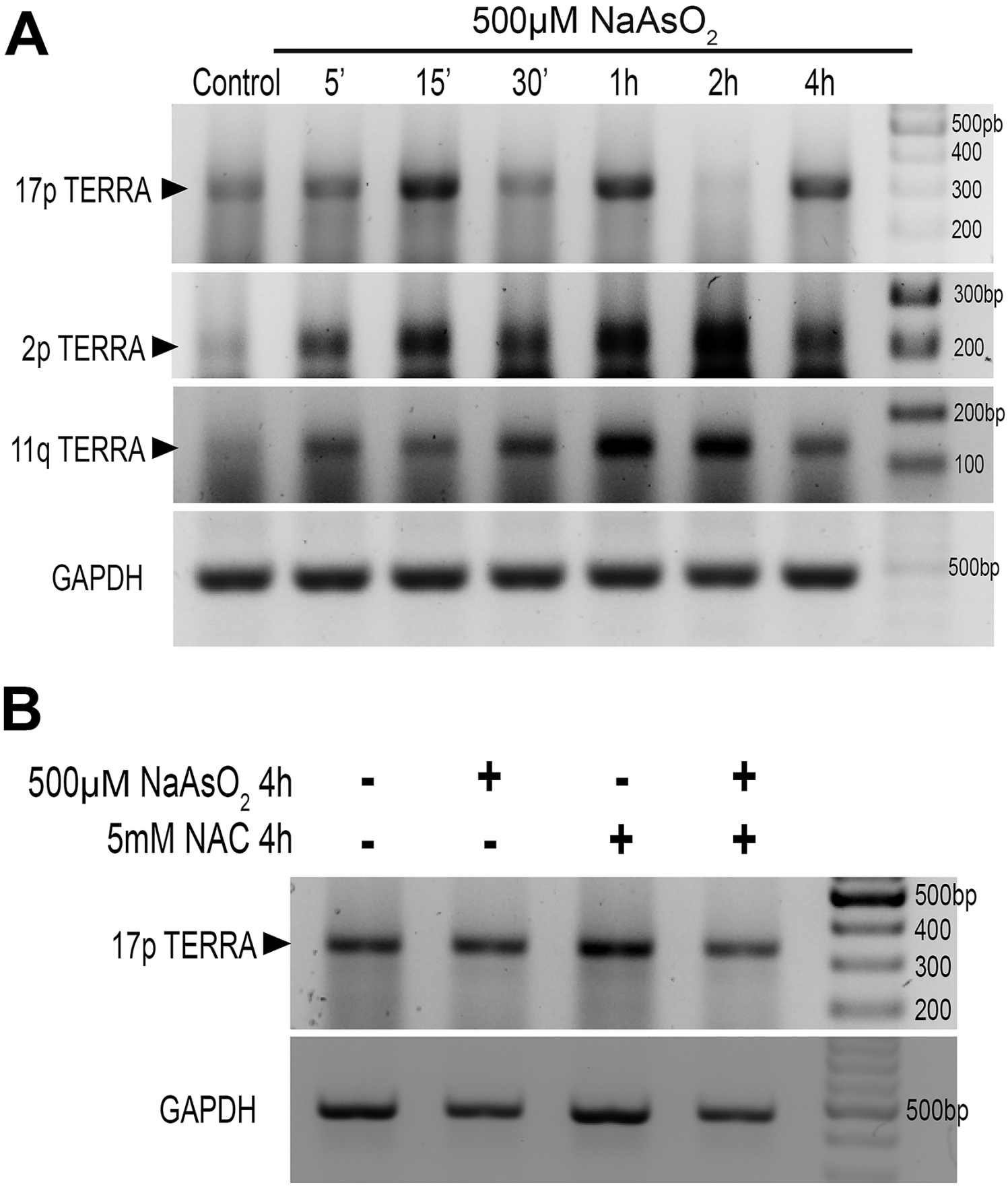
A
500μM NaAsO2
Control
5'
15'
30'
1h
2h
4h
17p TERRA
2p TERRA
11q TERRA
GAPDH
500pb
400
300
200
300bp
200
200bp
100
500bp
B
500μM NaAsO2 4h
5mM NAC 4h
17p TERRA
GAPDH
500bp
400
300
200
500bp

Figure 7

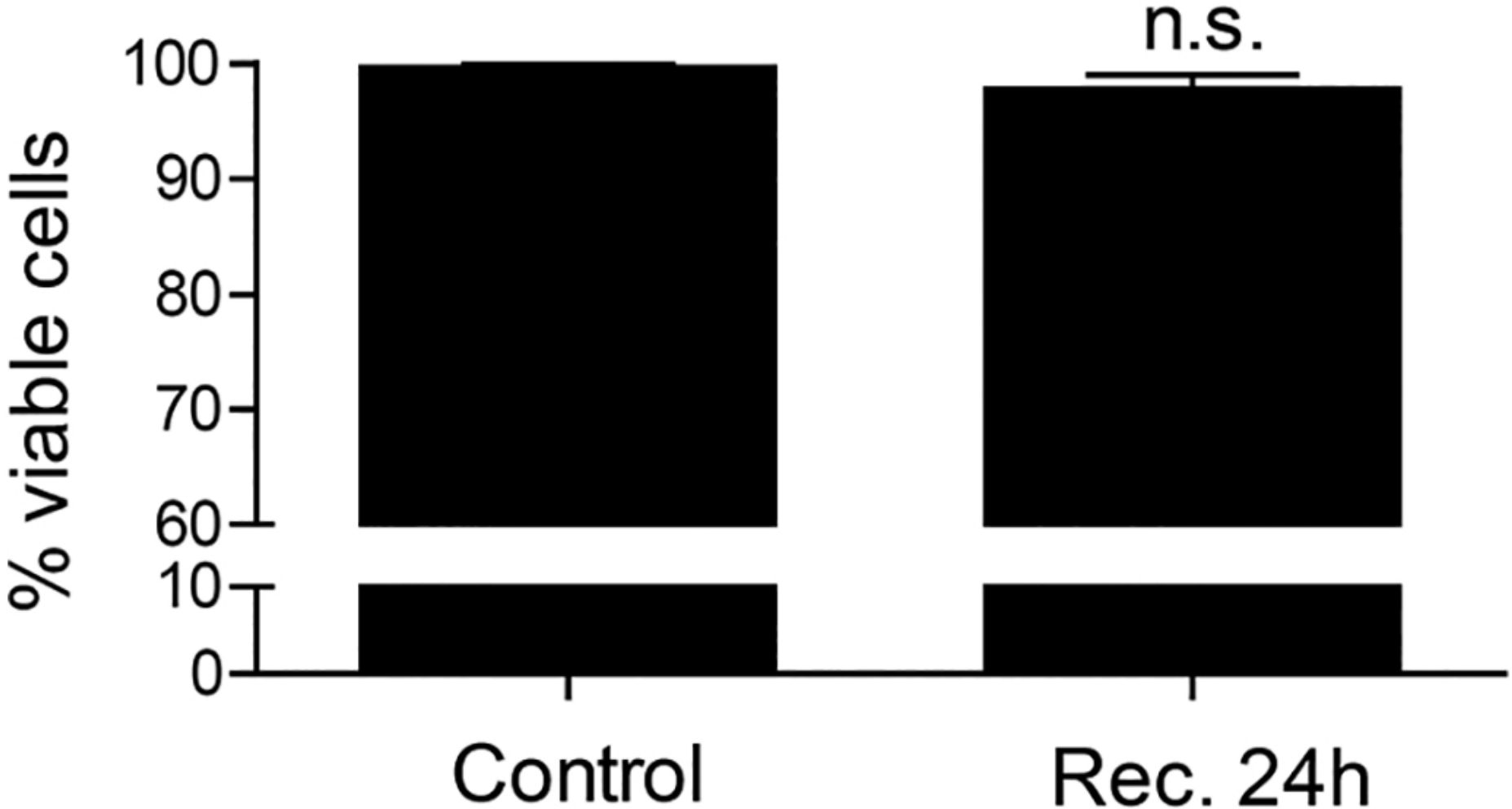

Figure 8